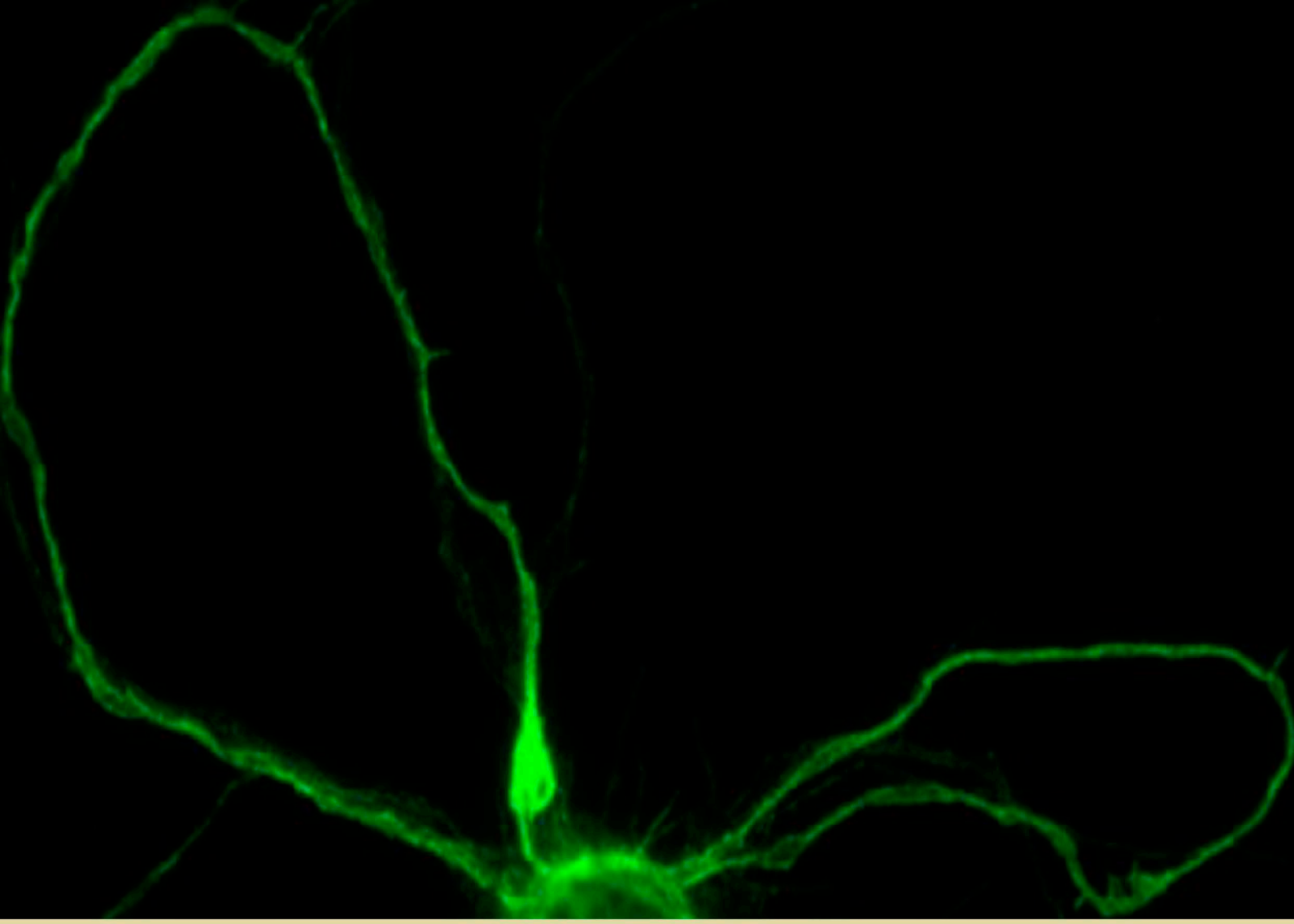

Rodolfo das Neves Águas

# 2B or not 2B that is the question about the synaptic proteasome in glutamatergic synapses

Tese de Mestrado em Investigação Biomédica, ramo de Neurobiologia,
orientada pela Professora Doutora Ana Luísa Carvalho e pela Professora Doutora Ana Cristina Rego
e apresentada à Faculdade de Medicina da Universidade de Coimbra

Julho 2018

· U C ·

Universidade de Coimbra

Rodolfo das Neves Águas

# 2B or not 2B that is the question about the synaptic proteasome in glutamatergic synapses

## Ter 2B ou não ter 2B: esta é a questão acerca do proteassoma sináptico nas sinapses glutamatérgicas

Dissertação apresentada à Faculdade de Medicina da Universidade de Coimbra
para obtenção do grau de Mestre em Investigação Biomédica – ramo Neurobiologia.

2018

· U C ·

Universidade de Coimbra

Cover legend: Rpt1-GFP-transfected mouse hippocampal neuron with 14 days *in vitro* labeled for GFP. The image is courtesy of Joana Ferreira.

This work was financed by the European Regional Development Fund (ERDF), through the COMPETE 2020 - Operational Programme for Competitiveness and Internationalisation and Portuguese national funds via FCT – Fundação para a Ciência e a Tecnologia, I.P., under projects POCI-01-0145-FEDER-007440 and PTDC/SAU-NEU/099440/2008.

Part of the work presented in this thesis has been published in the following article:

Ferreira, J. S., Schmidt, J., Rio, P., Aguas, R., Rooyakkers, A., Li, K. W., Smit, A. B., Craig, A. M., and Carvalho, A. L. (2015) GluN2B-Containing NMDA Receptors Regulate AMPA Receptor Traffic through Anchoring of the Synaptic Proteasome. *J Neurosci* **35**, 8462-8479

## DEDICATION

A vocês Nicole e Carolina dedico-vos este marco da minha vida académica que me desarmou, desmoldou e transformou enquanto pessoa e futuro cientista por serem uma prova constante e inabalável de que a persistência e a perseverança são o meio pelo qual se atinge o sonho.

Qual sonho? O passado talhou, o futuro dirá.

# EPIGRAPH

"Quando um homem que ainda não se encontrou tem todo o ar de ainda não se ter encontrado, bravo! Em vez de lástima merece respeito, é um sincero que nasce!

Ninguém no mundo se pode queixar de ter sido vítima da sua sinceridade. O que pode é cada um ficar surpreendido com o facto de a sua sinceridade o ter levado mais longe do que lho permite a sociedade. Este é outro caso.

Até hoje ainda nunca houve outro modo de cada um passar de uma idade para outra da sua vida a não ser pela sua sinceridade. Os modos de ludibriar essa passagem são sem conta. Mas a única maneira que existe no mundo para revelar cada um, a si e aos outros, está dentro de cada um mesmo, é a sua sinceridade.

A sociedade é uma mediania a transpor pessoalmente. Muitos sinceros caem-lhe nas malhas, não por terem sido sinceros, mas por incapazes de fazer frente à opinião pública, que acha destoante tudo o que é pessoal."

*Nome de Guerra* d' José Almada Negreiros

## TABLE OF CONTENTS

## LIST OF ABBREVIATIONS & CHEMICAL FORMULAS

**aa:** Aminoacid
**ABD:** Agonist-binding domain
**AMC:** 7-amino-4-methylcoumarin
**AMPA:** 2-amino-3-(3-hydroxy-5-methyl-isoxazol-4-yl) propionic acid
**AMPAR:** AMPA Receptors
**BCA:** Bicinchoninic Acid
**BSA:** Bovine Serum Albumin
**CaMKII:** Calcium/calmodulin-dependent protein Kinase II
**CNS:** Central Nervous System
**CP:** Core Particle
**CTD:** Carboxyl Terminal Domain
**DIV:** Days *In Vitro*
**DNA:** Deoxyribonucleic Acid
**DNase:** Deoxyribonuclease
**DOC:** Deoxycholic acid
**DTT:** (2S,3S)-1,4-bis(sulfanyl)butane-2,3-diol
**DUB:** Deubiquitinating enzyme
**E1:** Ub-activating enzyme
**E18:** Embryonic day 18
**E2:** Ub-carrier protein
**E3:** Ub ligase
**ECF:** Enhanced Chemifluorescence
**EDTA:** 2,2',2",2'"-(Ethane-1,2-diyldinitrilo)tetraacetic acid
**EGFP:** Enhanced GFP
**EPSC:** Excitatory Postsynaptic Current
**FRAP:** Fluorescence Recovery After Photobleaching
**GFP:** Green Fluorescent Protein
**GluN2B(-/-):** GluN2B KO
**HEPES:** 2-[4-(2-hydroxyethyl) piperazin-1-yl] ethanesulfonic acid
**kDa:** Kilodalton
**KO:** Knock-Out
**LTP:** Long-Term Potentiation
**LTD:** Long-Term Depression
**MAP2:** Microtubule Associated Protein-2
**MDa:** Megadalton
**MEM:** Minimum Essential Medium
**mEPSC:** miniature EPSC
**$Na_3VO_4$:** Sodium orthovanadate
**NaF:** Sodium fluoride
**NMDA:** N-methyl D-aspartate
**NMDAR:** NMDA Receptors
**NA:** Numerical aperture
**NTD:** N-Terminal Domain
**PBS:** Phosphate Buffered Saline
**PCR:** Polymerase Chain Reaction
**PMSF:** Phenylmethanesulfonyl fluoride
**PSD:** Postsynaptic Density
**PSD-95:** Postsynaptic Density protein-95
**PVDF:** Polyvinylidene difluoride
**ROI:** Region Of Interest
**RP:** Regulatory Particle

**Rpn:** Regulatory Particle non-ATPase

**Rpt:** Regulatory Particle Triple-A protein or Regulatory Particle Triphosphatase

**SAP90:** Synapse-Associated Protein-90

**SDS:** Sodium Lauryl Sulfate

**SDS-PAGE:** SDS-Polyacrylamide Gel Electrophoresis

**SEM:** Standart Error of the Mean

**SNS:** Synaptoneurosomes

**TBS:** Tris-Buffered saline

**TMD:** Transmembrane domain

**Tris:** 2-amino-2-(hydroxymethyl)-1,3-propanediol

**T-TBS:** TBS with 0.1% Tween 20

**TTX:** Tetrodotoxin

**Ub:** Ubiquitin

**UFD:** Ubiquitin Fusion Degradation

**UPS:** Ubiquitin-Proteasome System

**UV:** Ultraviolet

**VGLUT1:** Vesicular Glutamate Transporter 1

**WB:** Western Blotting

**WT:** Wild-Type

## ABSTRACT

NMDA receptors (NMDAR) are calcium-permeable transmembrane ion channels, which are key players in excitatory synaptic transmission. As tetrameric receptors, they are typically composed of two GluN1 subunits and two GluN2 subunits. In the hippocampus, GluN2BA and GluN2B are the two predominant forms of the GluN2 subunit family that are part of NMDA receptor composition. Both GluN2B subunits confer distinct properties to the NMDA receptors and could have distinct interacting partners which affect their subcellular localization. Through association with PSD-95, NMDA receptors are part of an organizing macromolecular complex, the postsynaptic density (PSD), which brings together downstream signaling transducers, like CaMKII, to NMDAR-mediated calcium influx. Memory, learning and brain development involve restructure at the level of synaptic function and strength. The proteasome has a role in these rearrangements by controlling temporally and spatially the PSD content. CaMKII binds to the GluN2B subunit and also mediates the recruitment of the proteasome into dendritic spines. Besides this structural role, CaMKII phosphorylates the proteasome subunit Rpt6 through which it influences the proteasome activity. Nevertheless, the connection between the GluN2B subunit and the proteasome is not well characterized.

In this thesis, we started by studying how NMDA receptors containing the GluN2B subunit influence the neuronal proteasome content, based on the fact that it was previously observed in our laboratory by quantitative proteome analysis that proteasome subunits, in particular α1, 3 and 6 and β1 and 2 subunits of the 20S proteasome, were decreased in PSDs of cortical neurons in the absence of GluN2B. Although we could not detect changes in the proteasome content in membrane fractions or synaptoneurosomes of GluN2B(-/-) neurons when compared to wild-type neurons, we measured the proteasome activity in GluN2B(-/-) and wild-type neurons, both *in vitro* by evaluating the 20S β5 activity and in live neurons by analysis of the UbG76V-GFP degradation reporter levels. We found that the proteasome activity was decreased in whole extracts obtained from neurons lacking the GluN2B subunit, compared to wild-type neurons. To understand whether the GluN2B subunit regulates the synaptic mobility of the proteasome, we made progress in implementing a FRAP assay to evaluate the synaptic mobility of the proteasome subunit Rpt1-EGFP, to allow us to study this aspect in the future. Finally, we found that the colocalization of the NMDAR GluN1 subunit and the Rpt3 proteasome subunit increased along development of cultured hippocampal neurons, and that their

synaptic localization showed a similar developmental pattern. These observations could indicate that localization of these proteins is interdependent.

Overall, these findings constitute a starting point for exploring further from a mechanistic point of view how the GluN2B subunit and the proteasome are connected.

## RESUMO

Os receptores NMDA são canais iónicos transmembranares permeáveis ao cálcio, os quais têm um papel fundamental na transmissão sináptica excitatória. Estes receptores são compostos por quatro subunidades, sendo que duas das quais são subunidades GluN1 e outras duas são subunidades GluN2. No hipocampo, as subunidades GluN2A e GluN2B são as duas formas dentro da família da subunidade GluN2 que integram os receptores NMDA. As subunidades GluN2A e GluN2B conferem propriedades diferentes ao receptor NMDA e podem até interagir com diferentes moléculas, o que afecta a localização subcelular dos receptores NMDA. Os receptores NMDA, através da sua associação com a PSD-95, fazem parte dum complexo macromolecular organizador, denominado densidade pós-sináptica, que aproxima os intervenientes de cascatas de sinalização, como a CaMKII, do cálcio que entra pelos receptores NMDA. A memória, a aprendizagem e o desenvolvimento do cérebro envolvem uma restruturação ao nível das função e eficácia sinápticas. O proteassoma tem uma função nessa restruturação através do controlo espacial e temporal do conteúdo proteico da densidade pós-sináptica. A CaMKII liga-se à subunidade GluN2B e também medeia o recrutamento do proteassoma para as espículas dendríticas. Além do seu papel estrutural, a CaMKII fosforila a subunidade Rpt6 do proteassoma influenciando deste modo a actividade do proteassoma. Contudo, a relação entre a subunidade GluN2B e o proteasoma foi até agora pouco estudada.

No decurso desta tese, testámos se os receptores NMDA contendo a subunidade GluN2B influenciam a quantidade de proteassoma sináptico, baseados num estudo anterior do nosso laboratório em que foi observado, por análise proteómica quantitativa, que algumas subunidades do proteassoma, especificamente as subunidades α1, 3 e 6 e β1 e 2, estavam diminuídas nas densidades pós-sinápticas de neurónios corticais quando a subunidade GluN2B está ausente. Embora não tenhamos detectado alterações nos níveis de proteassoma entre neurónios GluN2B(-/-) e GluN2B(+/-), quer em extractos membranares quer em sinaptoneurosomas, avaliámos a actividade do proteassoma em ambos os genótipos quer medindo *in vitro* a actividade da subunidade β5 do proteassoma 20S quer analisando em neurónios vivos os níveis do repórter de degradação UbG76V-GFP. Deste modo, verificámos que a actividade do proteassoma está diminuída em extractos totais obtidos de neurónios que não contêm a subunidade GluN2B, quando comparados com neurónios GluN2B(+/+). Com o propósito de perceber se a subunidade

GluN2B regula a mobilidade sináptica do proteassoma, fizemos alguns progressos na implementação de um ensaio de FRAP para a avaliação da mobilidade sináptica da subunidade Rpt1-EGFP, para que utilização num futuro próximo. Por fim, verificámos que a co-colocalização de ambas as subunidades GluN1 e Rpt3 aumenta ao longo do desenvolvimento de neurónios do hipocampo, e que a localização sináptica de ambas apresenta aumentos nos mesmos momentos temporais do desenvolvimento neuronal. Logo, estas observações podem indicar que a localização destas proteínas é inter-dependente.

Em suma, estas descobertas constituem um ponto de partida para estudar de um ponto de vista mecanístico como a subunidade GluN2B e o proteassoma estão associados.

# 1. INTRODUCTION

## 1.1. SYNAPSES

Synapses are the functional unit of the nervous system where communication between neurons takes place. These specialized cell-cell junctions are made up of pre- and postsynaptic compartments where, generally, an electrical signal is converted into a chemical one and this chemical signal turns back into an electrical one allowing the nerve impulse propagation along neurons. Inter-neuron chemical communication depends on a neurotransmitter system [1]. In detail, after an action potential reaches the presynaptic terminal neurotransmitter-containing vesicles fuse with the presynaptic membrane releasing their content into the synaptic cleft. This mechanism is triggered by an abrupt rise in cytosolic calcium ($Ca^{2+}$) concentration as a consequence of the depolarization-induced opening of presynaptic $Ca^{2+}$ channels. Subsequently, the binding of the neurotransmitters to their corresponding receptors on the postsynaptic membrane brings about their activation triggering a postsynaptic potential [2]. Synapses can be considered excitatory or inhibitory with the former ones culminating on the depolarization of postsynaptic membrane and increase of the membrane potential beyond the threshold dictating the generation of an action potential and its propagation on the postsynaptic neuron. On the contrary, inhibitory synapses lead to the hyperpolarization of the postsynaptic potential, decreasing it to values distant from the threshold for the generation of an action potential, and impeding propagation of electrical signals on postsynaptic neurons [3].

Moreover, to guarantee that synapses get properly formed, an accurate targeting of pre- and postsynaptic terminals is needed, a process that occurs during development and can be fine-tuned in response to learning [4].

## 1.2. GLUTAMATERGIC SYNAPSES

Glutamate is a neurotransmitter that acts on most of the excitatory synapses in the central nervous system (CNS). Its action occurs after glutamate gets released presynaptically and bound specifically to its receptor on the postsynaptic membrane transducing the excitatory signal into intracellular responses [3]. But for this to occur, glutamate receptors, being transmembrane proteins, need to be integrated and anchored in the postsynaptic membrane of the neuron, more particularly in dendritic spines, which

are tiny protuberances projected from the surface of dendrites. This presupposes the existence of molecular interactions between glutamate receptors and a membrane specialization, known as postsynaptic density (PSD), involved in the clustering of postsynaptic receptors at the synaptic surface and required for the assembly of the postsynaptic signaling machinery. In this way, a bridge is created between synaptic structure and function that allows rapid and efficient signal transduction. Besides this, other features confer highly compartmentalized (i.e. synapse-specific) postsynaptic signal processing like the unique morphology of dendritic spines, a head-shaped structure separated by a neck, of various length and width, from the dendritic shaft [3]. This latter neuronal domain – the dendritic shaft - is where inhibitory synapses, for example GABAergic, are usually found.

### 1.2.1. Postsynaptic densities

Located on the head of dendritic spines, directly opposed to the active zone in the presynaptic terminal, there is a microdomain, referred to as PSD, which contains scaffolding and signaling proteins connected structurally and functionally to postsynaptic glutamate receptors and trans-synaptic adhesion molecules [5][6]. Therefore, the PSD plays an essential role in localizing, organizing and stabilizing the glutamate receptors and adhesion molecules in the postsynaptic membrane conferring that the presynaptic release sites are aligned precisely with the neurotransmitter receptors on the postsynaptic terminal. Moreover, the PSD makes the postsynaptic signal transduction intrinsic to neuronal transmission rapid and efficient because signal transduction proteins are concentrated in the PSD and in close proximity spatially to glutamate receptors that activate downstream pathways through these signal transduction proteins [6]. The PSD is an exclusive feature of axodendritic glutamatergic synapses, which based on this structural characteristic are termed asymmetric synapses, in contrast to inhibitory ones which are designated symmetric, due to the fact this electron-dense thickening is not so noticeable [7] (Figure 1A).

Amongst the molecular postsynaptic proteome, calcium/calmodulin-dependent protein kinase II (CaMKII)α and -β and postsynaptic density-95 (PSD-95) [also known as synapse-associated protein 90 (SAP90)] have been identified as the most abundant proteins in PSD [5][8]. The PSD-95 is a protein containing PDZ domains which allow the formation of multiple protein-protein interactions in the PSD. One of PSD-95 interaction partners is the C-terminal tail of GluN2 subunits of NMDA receptors

(NMDAR) [9][10] (Figure 1B). This interaction gets relevance when the NMDAR become synaptic. During synapse formation, PSD-95 moves early into synapses when compared to NMDAR. Therefore, prior to NMDAR recruitment the PSD-95 clusters form a scaffold with other scaffolding proteins, to which NMDAR gets attached once it gets recruited to newly formed postsynaptic densities [11].

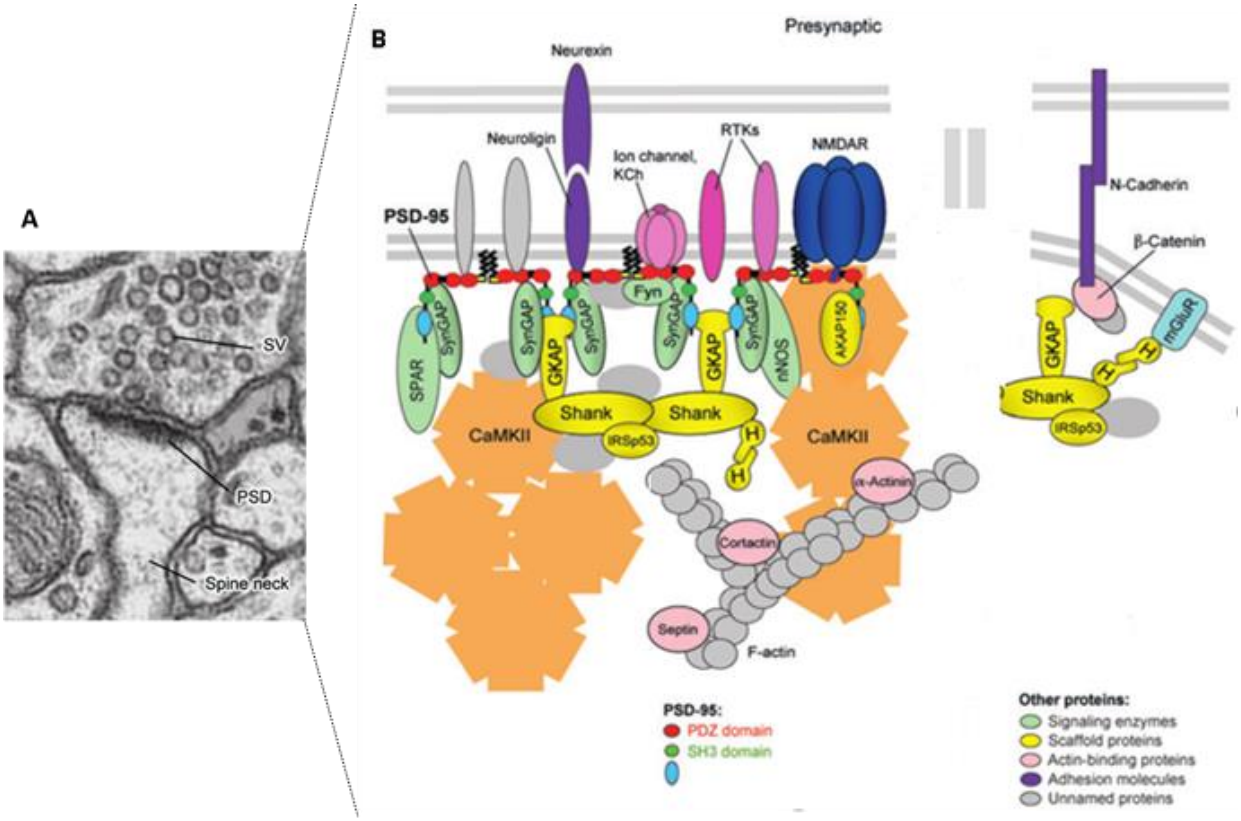


**Figure 1. Postsynaptic density (PSD) in glutamatergic synapses. (A)** Electron micrograph of an axodendritic synapse, where it is possible to identify a presynaptic terminal with synaptic vesicles (SV) and a postsynaptic terminal, rightly opposed to the presynaptic terminal, with an electron-dense thickening at the tip of the dendritic spine named PSD. Excitatory synapses are known to have this prominent ultrastructural feature, which distinguish them from inhibitory ones. **(B)** Simplified scheme of a PSD, depicting several proteins that compose this multifunctional specialization of the postsynaptic membrane, with PSD-95 and CaMKII being the most abundant. PSD components range from cell surface receptors, cell adhesion molecules, signal transduction proteins to cytoskeletal and scaffolding proteins. PSD-95 is a scaffolding protein, which through their PDZ-domain modular structure, interacts with multiple proteins. NMDAR, specifically the C-terminal tail of GluN2 subunit, is one of the proteins interacting with PSD-95 and, by the means of that interaction, PSD-95 tethers NMDAR to actin cytoskeleton. PSD-95, through a mesh-like matrix of scaffolding proteins, organizes the PSD into signaling macromolecular complexes, which bring together downstream signaling molecules, like CaMKII, to glutamate receptors. PSD-95 interacts with neuroligin, which in turn interacts with neurexin. That trans-synaptic complex justifies partly the correct alignment between pre- and postsynaptic terminals. (A) and (B) are, respectively, reproduced and adapted with permission from the Annual Review of Biochemistry, Volume 76, © by Annual Reviews, http://www.annualreviews.org.

CaMKII is a signal transduction protein translocated and concentrated on the PSD upon synaptic activity that has a key physiological role in the molecular mechanisms underlying memory and learning [12]. In neurons where the major neuronal isoforms of CaMKII are the α and β, this dodecameric enzyme can be found in either CaMKIIα homomultimers or CaMKIIα and –β heteromultimers [13] (Figure 2A). Each of the 12 subunits contains a catalytic kinase domain, a regulatory segment and a self-association domain [14]. Before being activated by $Ca^{2+}$/ calmodulin, the kinase domain (S-site) of CaMKII is autoinhibited by part of its regulatory segment that resembles protein substrates. Thereby the S-site is blocked in a pseudosubstrate manner inhibiting enzyme activity. CaMKII is further stabilized in its inactive state by capturing the T286 phosphorylation site in a hydrophobic pocket (T-site) of CaMKII structure. Once $Ca^{2+}$/ calmodulin binds to CaMKII, which binding region is partially shared with the pseudosubstrate region, the S-site is no longer blocked. Moreover, the CaMKII remains active beyond the $Ca^{2+}$ spike. Following $Ca^{2+}$/ calmodulin binding, conformational changes in CaMKII expose T286 (T287 in CaMKIIβ) allowing intersubunit phosphorylation on that threonine, which consequently frees the T-site to bind, for example, the C-tail of the GluN2B subunit. Either the T286 phosphorylation or the binding to GluN2B subunit renders the enzyme to a persistently active state, i.e. in these conditions the CaMKII activity is independent of $Ca^{2+}$ [15] (Figure 2B). Of note, CaMKII has more binding partners besides NMDAR [16][17]. In fact, apart from kinase activity either CaMKIIα or -β can have a structural role, respectively, in scaffolding the proteasome in PSDs [12] and bundling actin filaments intrinsic to maintenance of dendritic spine morphology [18]. Other PSD proteins, not so abundant as the last ones

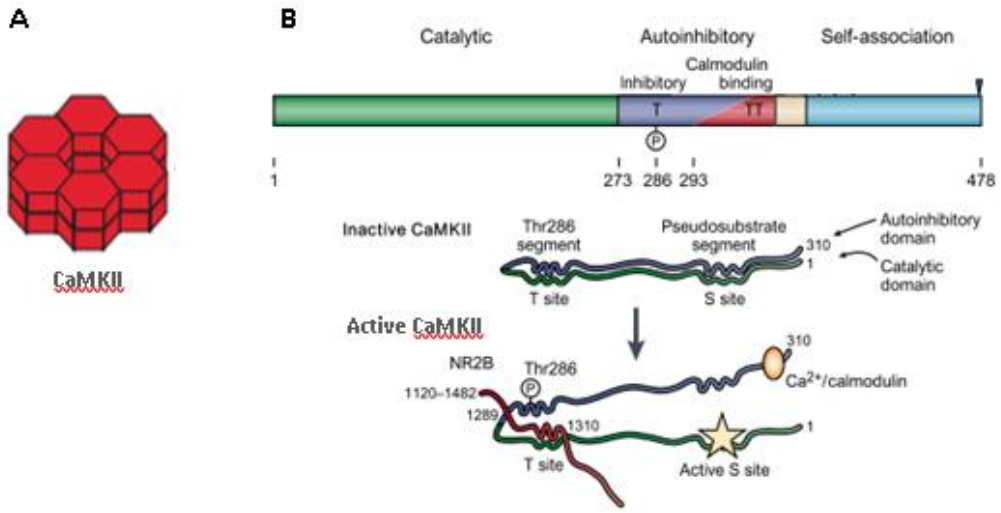

Figure 2. **CAMKII structure and inactive/ active state representation. (A)** CaMKII is a 12-subunit protein. Tri-dimensionally those subunits arrange themselves in a two-stacked structure with six subunits per stack. In the brain CaMKII exists mainly in two isoforms, α and β. Given that, CaMKII can assume either CaMKIIα homodimers or CaMKII α and -β heteromultimers. **(B)** From a cellular standpoint, CaMKII is a kinase, which has a major importance in transducing increases in $Ca^{2+}$ levels into biochemical responses subjacent to synaptic transmission. CaMKII, through those cellular responses, could also be involved in learning and memory. Nevertheless, CaMKII is inactive under basal conditions. CaMKII is kept in this state by 1) an interaction, in a pseudo-substrate manner, of a segment of the autoinhibitory domain to the substrate- and ATP-binding site (S-site) and 2) sequestering one of the regulatory phosphorylation sites of CaMKII, namely Thr286, in a hydrophobic pocket (T-site). Once $Ca^{2+}$/ calmodulin binds to CaMKII, CaMKII becomes active. When CaMKII gets activated, conformational changes happen which exposes Thr286 to phosphorylation. Thr286-phosphorylated CaMKII can be persistently active, even after $Ca^{2+}$ levels fall to baseline levels. Different factors control how long CaMKII stays in a persistently active state, like 1) interaction with the C-terminal domain of NMDA GluN2B; 2) phosphatase activity and 3) $Ca^{2+}$ elevation frequency and intensity. However, CaMKII functions go further than its kinase activity, for example, CaMKII can act as a scaffold to proteasomes or be involved in spine morphology through destabilization and remodeling of actin cytoskeleton.
(A) Reproduced fromMerrill M. A.& Chen y. & Strack S. & Hell J. W.; Trends in Pharmalogical Sciences; 26: 645-653; 2005. (B) Adapted from Lisman J. & Schulman H. & Cline H.; Nature Review Neuroscience; 3: 175-190; 2002.

mentioned, include Homer1c that functions as an adapter complex constitutively expressed in PSD which interacts with Group I metabotropic glutamate receptor, scaffolding it at PSD [19].

The dynamics of synaptic CaMKII is extended to other PSD proteins since the PSD architecture is dynamically controlled and adjusted in structure and composition to respond to the requirements of synaptic activity with the proteins being redistributed to or away from synapses or even turned over locally through the ubiquitin-proteasome system [5][7].

### 1.3. UBIQUITIN-PROTEASOME SYSTEM

The ubiquitin-proteasome system (UPS) is involved in the selective proteolysis for controlling temporally and spatially the cellular proteome and its quality in the eukaryotes [4]. Generally, this system comprises two consecutive and discrete steps: (1) the conjugation of ubiquitin (Ub) moieties to the protein to be proteolysed, known as the ubiquitination, and (2) the degradation of the tagged protein by the self-compartmentalized multiprotein complex, the 26S proteasome [20].Covalent conjugation of Ub, a highly conserved evolutionarily 76-residues polypeptide, to the target protein is catalyzed by the sequential action of three enzymes, E1, E2 and E3, with ATP consumption in the Ub conjugation reaction [21]. Firstly, the Ub-activating enzyme (E1) activates free Ub in an ATP-dependent manner. Activated Ub is then transferred to an E2, commonly referred as Ub-carrier protein. Finally, either Ub is directly attached to a target

protein, which is facilitated by an ubiquitin ligase E3, or an E3 first accepts Ub from E2s and then covalently attaches it to a target protein (Figure 3). The selectivity of protein degradation lies mainly at the Ub conjugation, where E3s, as they recognize specific recognition motifs on protein substrates, play a key role in determining which protein is targeted for proteasome-mediated degradation [4],[21]. Ub tags can mark proteins to different cellular destinations depending on whether the protein is monoubiquitinated, multiple monoubiquitinated or polyubiquitinated and also at which lysine(s) (Lys) residue the ubiquitin is bound to [22]. To signal a protein for degradation in the proteasome, a polyUb chain of at least four Ub moieties should be attached in such a way that Ub moieties bind to the ε-$NH_2$ group of an internal Lys residue of Ub, specifically the Lys48. The polyUb chain can be made by attaching a free Ub on a previously conjugated Ub or an unbound polyUb chain can be transferred *en bloc* to a substrate [23].

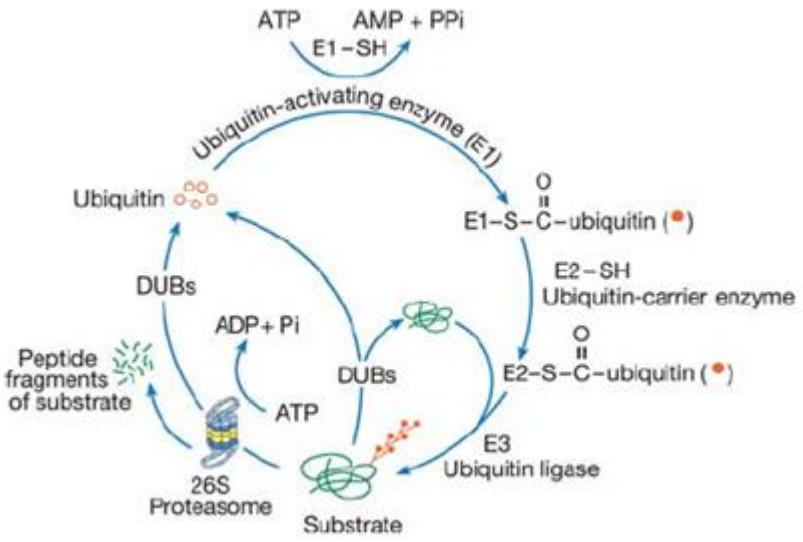


**Figure 3. Ubiquitin-proteasome system.** This scheme illustrates the pathway by which a protein is firstly tagged with ubiquitin and, ultimately, degraded to short peptides that vary in length from 4 to 25 residues in the 26S proteasome. Firstly, free ubiquitin (represented by red circumferences) is activated by ubiquitin-activating enzyme (E1) in an ATP-dependent manner. Then, the activated ubiquitin (represented by red circles) is transferred to the ubiquitin-carrier enzyme (E2), and from this one to the ubiquitin ligase (E3), which mediates the conjugation of ubiquitin to the protein to be proteolysed.

After conjugation of one ubiquitin to a protein , specifically on lysine 48, a series of ubiquitin molecules, minimum of three, link through the previous ubiquitin moiety forming a polyubiquitin chain, which is the signal recognized by the 26S proteasome for a protein to be proteolysed. The polyubiquitinated proteins culminate in the ATP-dependent proteolysis in the 26S proteasome however the polyubiquitin chain is not degraded along with the protein. The recycling of the polyubiquitin chain is executed by deubiquitinating enzymes (DUBs), which can also prevent a protein to be erroneously degraded.

Reproduced, with permission, from Hedge, A. N.; *Learning Memory*, 17: 314-327, 2010.

### 1.3.1. 26S proteasome

The 26S proteasome is made by the 20S proteasome, the core particle (CP) with protease activity, and the 19S regulatory particles (RP) at one or both ends of it. The assembly of 26S proteasome' components is ATP-dependent. The 26S proteasome is an approximately 2.5MDa complex with the 20S proteasome weighting 720kDa and each RP 890kDa, according to scanning-transmission electron microscopy [24].

After target proteins are tagged with a polyUb chain, they are directed toward the 26S proteasome or, on the contrary, it is the 26S proteasome itself that adjusts its cellular localization in the direction of those proteins. Generally, the 26S proteasome recognizes the polyUb chain of a tagged polypeptide, cleaves the tag via its deubiquitinase activity, unfolds the protein and, ultimately, catalyzes the degradation of them into short peptides [25] from 4 amino acids (aa) to 25 residues long [26].

In the eukaryotes, the 20S CP is made up of four stacked heteroligomeric rings with the inner rings, which contain seven distinct β subunits, flanked on top and bottom by a ring of seven different α subunits. Tridimensionally, the stoichiometry [(α1-α7)(β1-β7)(β1-β7)(α1-α7)] results in a hollow barrel-shaped complex that harbors, facing inward the self-compartmentalized chamber [24], some β subunits with proteolytic activity [20]. The β1-, β2- and β5-subunits are the ones responsible for that activity, each with its own specificity, chymotrypsin-, trypsin- and caspase-like, respectively, which has been determined by model peptide substrates [26]. These specificities result in preferential cleavage of a peptide bond after hydrophobic, basic and aspartic residues located N-terminally on the tagged protein with regard to β1-, β2- and β5-subunits, respectively [26].

Even though the 20S proteasome is the component responsible for protein degradation, due to the narrowness of the 20S CP's channel only unfolded proteins fit through this channel, which gives access to the catalytic compartment. Therefore, the 20S CP must be associated with other components capable of unfolding the target proteins [23]. The unfoldase activity is attributed to the 19S RPs, which is ATP-dependent. In fact, the 19S RPs contain six ATPases of the AAA family, designated Rpt1-6 for regulatory particle triphosphatase or regulatory particle triple-A protein, which constitute the molecular motor of the proteasome [27]. Those ATPases use the energy from ATP hydrolysis to open the 20S CP's channel and to unfold the substrate, facilitating the translocation of the unfolded peptides into the 20S proteasome. The gate is blocked by

the N-tails of α-subunits and its opening and closing are controlled by multiple Rpt-α subunits interactions [28]. The ATPases, together with three non-ATPases Rpn1, 2 and 13, make up one of the subcomplexes of the 19S RPs, named the base. Apart from that subcomplex, the 19S RPs have the lid, conventionally the subcomplex distally located in the 19S proteasome, that consists in nine regulatory particle non-ATPase (Rpn) subunits, Rpn3, 5-9, 11, 12 and 15, which recognize the polyUb chain from substrates to be degraded and remove the polyUb chain through deubiquitination [28]. The lid is required for ubiquitin-dependent degradation; however, the 20S proteasome associated with the base is sufficient for degradation of non-ubiquitinated target proteins [24].

### 1.4. GLUTAMATE RECEPTORS

Glutamate receptors are transmembrane proteins integrated in the postsynaptic site of glutamatergic synapses. Binding of these receptors to glutamate initiates a cascade of intracellular signaling pathways [29]. These receptors can be grouped into ionotropic or metabotropic receptors, the latter being receptors coupled to G-proteins, whose activation translates functionally in a slower synaptic response than ionotropic glutamate receptor-mediated response [30]. The ionotropic glutamate receptors are further categorized into three families: NMDAR, AMPA receptors (AMPAR) and kainate receptors. The non-NMDAR, which enclose the AMPAR and kainate receptors, are voltage-independent ion channels that upon glutamate activation generate the initial short-lasting and fast component of the excitatory postsynaptic current (EPSC) [31]. On the contrary once activated, NMDAR generate a slower and long-lasting EPSC with a considerable $Ca^{2+}$-component. $Ca^{2+}$ entry through NMDAR initiates several intracellular pathways [29], involved for example in synapse formation, modification and elimination [31].

Since NMDAR ion channel is blocked within the ion channel pore by extracellular $Mg^{2+}$ at resting membrane potential, NMDAR permeation to $Na^{+}$, $K^{+}$ and $Ca^{2+}$ requires the depolarization for relief of the $Mg^{2+}$ blockade to be paired with the binding of glutamate and the co-agonist glycine (or D-serine) (Figure 4A). Given these activation requirements, NMDAR are considered both voltage- and ligand-dependent, which is a distinctive feature of NMDAR compared to other glutamate receptors. Interestingly, given the fact that $Mg^{2+}$ blockade is only released at depolarized membrane potentials, NMDAR act as coincidence detectors, i.e. the NMDAR are exclusively activated when presynaptic release of glutamate and postsynaptic depolarization occur concomitantly [32]. In terms of subunit composition, NMDAR is a tetrameric complex typically

composed of two dimers of the GluN1 subunit and two dimers of the GluN2 subunit. The GluN2 subunit can assume four distinct forms, GluN2A, GluN2B, GluN2C and GluN2D, all of them encoded by different genes [29] (Figure 4B). Depending on the GluN2 subunit identity, NMDAR reveal different pharmacological and electrophysiological properties and even different interacting partners, which influence their subcellular localization. In

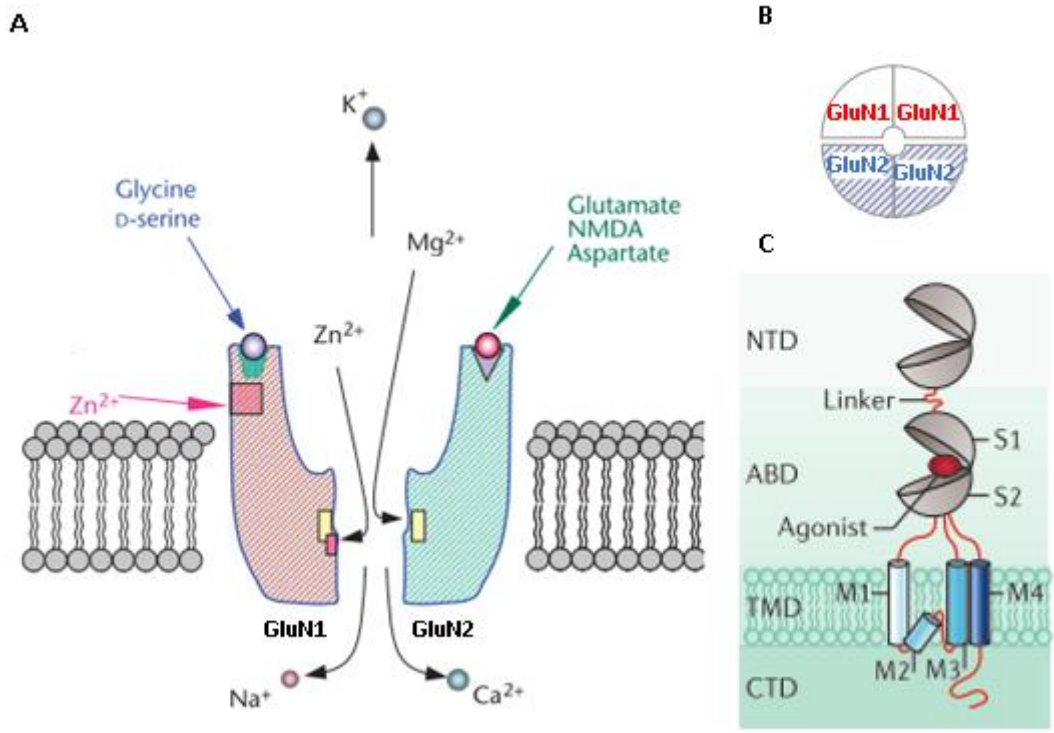


**Figure 4. NMDA receptor agonists & modulators, composition and modular architecture. (A)** NMDAR, together with kainate and AMPA receptors, belong to a class of ligand-gated channel receptors permeable to cations, named ionotropic receptors. Besides these receptors are cation-permeable, at basal conditions $Mg^{2+}$ binds inside NMDAR ion channel impeding its permeability to cations. This blockage makes NMDAR dependent of voltage since membrane depolarization relieves NMDAR from $Mg^{2+}$ turning it permeable to $Na^{+}$, $K^{+}$ and $Ca^{2+}$. Furthermore, NMDAR only gets fully activated when the four NMDAR agonist-binding sites bind to their respective agonists (glycine or glutamate). Specifically, GluN1 subunit binds glycine (or D-serine) while GluN2 subunit binds glutamate. $Zn^{2+}$ binds to NMDAR and, through this, modulates NMDAR function. $Zn^{2+}$ is only one example of NMDAR allosteric modulators. These modulatory ligands show specificity towards certain subunits. $Zn^{2+}$ acts on GluN1-GluN2A receptors, while ifenprodil acts on GluN1-GluN2B ones. These characteristics (permeability and modulatory ligands), along with NMDAR channel kinetics, make NMDAR unique amongst glutamate receptors. **(B)** In terms of composition, NMDAR can be composed of subunits from three subfamilies - GluN1, GluN2 and GluN3- to a total of four subunits. As obligatory subunit, GluN1 has to be part of NMDAR. NMDAR assemble as a dimer of dimers, with its favored conformation being the one shown. Generally, NMDAR are GluN1/ GluN2 heterodimers, with GluN2 varying, for example, between GluN2A and GluN2B through development and activity. **(C)** Each NMDAR subunit is organized into domains – N-terminal domain (NTD), agonist-binding domain (ABD), transmembrane domain (TMD) and intracellular C-terminal domain (CTD). Given NMDAR nature as an ion channel, TMD, with its three transmembrane domains – M1, M3 and M4 – and a re-entrant loop – M2 – is responsible for lining the ion channel. With NTD and CTD involved in receptor regulation, channel gating mechanism and subsequently NMDAR activation is dependent of ABD and TMD. (A) and (B) are adapted, with permission, from Cull-Candy S.; Encyclopedia of Life Sciences, 2007 and (C) is reproduced, with permission, from Paoletti P. & Bellone C.& Zhou Q.; Nature Reviews Neuroscience; 14:383-400, 2013.

the hippocampus and cortex, GluN2A and GluN2B subunits are the predominant subunits within the GluN2 subunit family. Nevertheless, their predominance varies during development, with GluN2B subunit-containing NMDAR being partially exchanged by GluN2A-containing ones postnatally. Specifically, this subunit switch coincides in time with synapse maturation, circuit refinement and learning processes [29][30]. Topologically, each NMDAR subunit consists of an N-terminal domain (NTD), an agonist-binding domain which binds glycine (or D-serine) in the obligatory GluN1 subunit and glutamate in the GluN2 subunit, four membrane-inserted domains that line the ion channel pore and an intracellular C-terminal domain (CTD) [33] (Figure 4C). While the NTD is involved in subunit assembly the cytoplasmic CTD, being of considerable length, has different motifs which, depending upon the interactor, could modulate the receptor cycling in and out of synapses, its localization in the PSD or signaling pathways associated [29]. Still on NMDAR localization respect, it is important to note that NMDAR, besides being expressed in postsynaptic sites, are also found in presynaptic sites from where they can influence excitatory synaptic strength [29].

### 1.5. GluN2B-containing NMDAR and NMDAR in general in disease-context

Glutamate is an excitatory neurotransmitter, which binds to the GluN2 subunit of NMDAR contributing in part to the activation and function of these ion channels [34]. In disease scenarios, which could be characterized by prolonged extracellular glutamate concentrations, glutamate has detrimental effects on neuronal health. These effects occur via $Ca^{2+}$ influx and culminate in neuronal death, being NMDAR the main channel through which $Ca^{2+}$ enters and kills neurons [35]. This is a phenomenon named excitotoxicity. However excitotoxicity is only one side of NMDAR activation, since NMDAR is also involved in neuroprotection [29]. Some hypotheses were built to explain the dual nature of NMDAR activation. Initially excitotoxicity was attributed to the volume of $Ca^{2+}$ influx, where intense NMDAR activation, with its matching evoked $Ca^{2+}$ level, would be prejudicial to neurons [35]. This hypothesis did not provide enough explanation when extrasynaptic NMDAR role in the context of disease had started to be taken in consideration or even considering the fact that interestingly intense synaptic NMDAR activation is neuroprotective and well tolerated by hippocampal neurons [36]. From then on, the hypotheses went on to consider the NMDAR itself, from its location to the GluN2 receptor composition, as a justification for the dual nature. NMDAR location seems to determine whether neurons are more vulnerable or not to cell death by being coupled to

different $Ca^{2+}$-dependent signaling pathways. This has been seen as synaptic NMDAR being associated to neuroprotection, while extrasynaptic NMDAR seem to be coupled to cell death pathways [36]. Furthermore, GluN2 subunit identity, more specifically GluN2 CTD, seems to have a contribution on the matter of vulnerability to cell death. If a NMDA receptor has GluN2B subunits in its composition NMDAR activation will render neurons susceptible to cell death, which is higher than when NMDAR is composed of GluN2A subunits [37]. This observation can seem a bit contradictory on the light of NMDAR location effect over neuronal health, since GluN2B-containing NMDAR can also be synaptically localized and neuroprotection-related [38]. Moreover, in the same study it was observed that when neurons were exposed to high doses (100 μM) of NMDA the influence of GluN2B-containing NMDAR over vulnerability to cell death was lost. This suggested that possibly the GluN2 identity would affect excitotoxicity in context of chronic exposure to glutamate [37]. Upon so many determinants to excitotoxicity surrounding NMDAR dysfunction, further research will be of extreme importance to fully understand how to modulate and potentiate, in disease scenarios, NMDAR activation towards neuroprotection, while suppressing the harmful effects of excitotoxicity. Along the years NMDAR has been associated to many neuropathological disorders, which include conditions resulted from acute NMDAR activation like stroke and traumatic brain injury; schizophrenia; and chronic neurodegenerative diseases like Huntington's disease, Parkinson's disease and Alzheimer's disease [35], [39], [40]. While some of these diseases might be characterized by neurons becoming vulnerable to endogenous levels of NMDAR activity [35], in others like schizophrenia the NMDA hypofunction might be the rationale behind the disease [39]. Given the scope of this thesis, the UPS could not be left out of a disease-context and, in fact it has observed its contribution in neurodegenerative disorders including Alzheimer's disease, Huntington's disease, amyotrophic lateral sclerosis, Parkinson's disease and neurodevelopmental disorders, like autism. Some of these diseases are characterized by accumulation of intracellular ubiquitin-positive protein inclusions, which may presuppose malfunction of protein degradation mechanisms including proteasome-dependent ones [41], [42]. As it would be seen in the subsection 1.7, NMDAR and the proteasome seem to be mechanistically related in physiological conditions [43]. Therefore, the aforementioned neuropathological disorders can benefit directly from comprehending better the extent of NMDAR-proteasome connection and if this helps explaining some hallmarks of those disorders.

### 1.6. NMDAR IN SYNAPTIC PLASTICITY

During learning, memory and brain development synapses are subjected to various patterns of neuronal activity. Synapses have mechanistically different forms of plasticity which allow them to, on one hand, adapt their efficacy in conformity to neuronal activity and, on the other, self-regulate the activity of a neuron or neuronal circuit if neurons get either hyperexcited or extremely inactive [44]. Long-term potentiation (LTP) and long-term depression (LTD) are classical (also known as Hebbian) forms of plasticity which are characterized for being synapse-specific [45]. LTP translates into a strengthening of synaptic transmission when activation of presynaptic side is combined with a strong postsynaptic depolarization. Experimentally this strong depolarization could be induced either pharmacologically or through a high-frequency tetanus, if this surpasses the LTP induction threshold, or with a weak tetanus when this stimulus is paired with a strong one [46]. On the contrary, LTD leads to the weakening of synaptic strength and could be induced with a low-frequency stimulus. In the CA1 region of hippocampus, both LTP and LTD are triggered by $Ca^{2+}$ that enters through NMDAR. Nevertheless, the direction of Hebbian plasticity has been hypothesized to be dependent on magnitude and duration of the NMDAR-mediated $Ca^{2+}$ influx or even the source of $Ca^{2+}$. So, in a simplified perspective, high and small NMDAR-mediated $Ca^{2+}$ influx will lead to LTP or LTD, respectively [45]. In an early phase of LTP, $Ca^{2+}$ activates CaMKII which consequently increases AMPAR insertion at the surface of synapse enhancing AMPAR-mediated current. On a later phase of LTP, synapses suffer a remodeling, where UPS is involved, to accommodate more receptors occurring a trans-synaptic growth of synapses [48]. This growth on pre- and postsynaptic sides of synapses, associated with the long-term condition of LTP, involves protein synthesis and gene transcription [44]. Either LTP and LTD work through positive feedback mechanisms which would impede neurons and neuronal connections from being continuously potentiated or depressed, respectively. Synaptic scaling and metaplasticity are forms of homeostatic plasticity, that through global negative feedback, counteract deregulated states of neuronal activity allowing neurons to continue functional. Synaptic scaling might cause alterations in the global neuronal strength, but not in the direction of the synaptic plasticity. These alterations happen either presynaptically in glutamate-releasing machinery as postsynaptically in the number or kinetics of NMDA receptors [45][49]. Metaplasticity works by comparison with previous events of synaptic plasticity altering plasticity thresholds. One clear example of metaplasticity happens during the development of the visual cortex, where

the continuous light exposure and stimulation alters the LTP-inducing threshold so the stimulus that once elicit LTP could not elicit LTP any longer or even favor LTD instead of LTP [45]. For instance, it has been studied that NMDAR-mediated metaplasticity could depend whether the neurons are mature or under development. During development, in the hippocampal neurons of CA1 region there is a partial switch from GluN2B-containing receptors to GluN2A-containing receptors [29][30]. Since GluN2A and GluN2B confer different properties – biophysical and localization - to NMDAR and they are thought to be associate to different downstream signaling pathways, therefore this can contribute to understand their involvement in different forms of plasticity [46][50]. Even if NMDAR are involved in synaptic plasticity mechanisms further investigation needs to done for clarifying the distinct contribution of NMDAR to each form of plasticity.

### 1.7. THE CAMKII-GLUN2B-PROTEASOME TRIAD

Many questions have puzzled the scientific community about the proteasome and how its proteolytic activity is translated into a functional role in the postsynaptic sites of glutamatergic synapses. Throughout the last decades, three molecular elements – $Ca^{2+}$/ CaMKII, GluN2B subunit and the proteasome – have emerged as key modulators of synaptic function. Moreover, several articles have pointed out advances about how each of the previously mentioned elements interacts with the others, what is the biological purpose behind these interactions and how they are affected by synaptic activity.

By 2003, it was already known that morphological remodeling of the PSD is accompanied with functional changes in synaptic strength, which is required for learning and memory [34],[35]. Also, ubiquitin-dependent mechanisms were found to be involved in synaptic function [36],[37]. However, it was still a mystery how the PSD remodeling responds to synaptic activity and if and how the ubiquitin-dependent mechanisms interconnect with the PSD remodeling.

Through pharmacological approaches either blocking or stimulating action potential generation by incubating neurons with tetrodotoxin (TTX), a $Na^+$ channel blocker, or bicuculline, a GABAergic antagonist, respectively, Ehlers, M.D. (2003) saw that activity regulates the abundance of postsynaptic proteins in a bidirectional manner, for example GluN2 subunits and CaMKII. Particularly, GluN2A and GluN2B subunits total abundance is, respectively, increased and decreased in active synapses, i.e. bicuculline-treated neurons, whereas upon synaptic blockade by TTX GluN2A and GluN2B subunits total abundance changes in opposite directions. Furthermore, CaMKII increases upon

treatment with bicuculline and decreases in TTX-treated neurons. Apart from abundance, turnover rates of different postsynaptic markers were also assessed and the GluN2A subunit half-life was unchanged with synaptic activity, while the GluN2B subunit half-life increased or decreased in synaptically inactive or active PSDs, respectively. The latter observation gives rise to the question of what change(s) occur in the GluN2B subunit that explain its half-life depending on the synaptic activity state. In addition, if the half-life of CaMKII does not change with synaptic activity, but its abundance is dependent on that, maybe its accumulation is due to trafficking of CaMKII in and out of the PSD. This had been supported with initial evidences from other studies [38],[39], but needs further research to dissect the key molecular players and their functional relevance. Since back then, one of the suggested hypotheses to explain the activity-dependent changes in PSD composition was the dynamic turnover of the PSD in response to activity [40],[41], and degradation via the ubiquitin-proteasome system was taken in account as a player in the PSD turnover. The levels of ubiquitin-conjugated proteins, in the presence of bicuculline and TTX, were altered, i.e. increased and reduced, respectively. Accordingly, the protein profile upon neuronal treatment with proteasome inhibitors mimicked the protein profile obtained with synaptic blockade and prevented activity-induced remodeling. Overall, this study [43] provided a bridge, beyond the electrical properties of the synapse, between activity and proteasome-mediated degradation, which culminates in the PSD remodeling.

Taking a step further, Barria A. and Malinow R. (2005) explored how the binding between active CaMKII and GluN2B subunit correlates with LTP, which is a form of synaptic plasticity involved in memory formation. CaMKII, upon being activated and translocated to dendritic spines, can bind to NMDAR, specifically it binds with high affinity to the C-tail of the GluN2B subunit and with low affinity to the GluN2A subunit [43],[44]. GluN2 subunit varies along the development of the hippocampus, with GluN2B prevalence over GluN2A subunit in the immature hippocampus being partially replaced by the GluN2A subunit in the mature animal [61]. In a period when GluN2B is dominant, between the early postnatal stage and adulthood, it was seen that LTP was significantly reduced by replacing the GluN2B for the GluN2A subunit, or even by reducing association between the active CaMKII and GluN2B subunit. Therefore, binding of CaMKII to GluN2B subunit is required for synaptic plasticity [50], at least in the immature hippocampus. In the adult hippocampus, despite the predominance of GluN2A subunit, GluN2B is still required to produce LTP. Even if sufficient $Ca^{2+}$ entry depends mostly on activation of dominant GluN1 and GluN2A-containing NMDARs, synaptic

inclusion of GluN2B subunit in NMDAR may be crucial to modulate downstream events, which include CaMKII binding to GluN2B subunit and the long-lasting CaMKII autophosphorylation in Thr286. Therefore, a cooperative role between GluN2A- and GluN2B-containing NMDAR seems to be required for LTP in adult hippocampus, but needs further elucidation. Functionally, the blockade of only 25% of GluN2B-CaMKII binding in adult mice (aged 4 to 6 months) affects the rate of acquisition of hippocampal-dependent spatial learning [62].

The proteasome is involved in protein degradation mechanisms by which there is a control of neuronal proteome subjacent to synaptic plasticity [43]. Through time-lapse imaging after KCl depolarization, it was shown that both 20S and 19S proteasome translocate from dendritic shafts into spines in an activity-dependent manner and the proteasome is functional in the spines. Besides the fact that KCl depolarization leads to activation of many voltage-gated channels, NMDAR activity seems to be specifically involved in the recruitment of the proteasome into spines and consequently associated to local degradation in spines. Using live cell imaging microscopy coupled to induced neuron depolarization, it was seen that the proteasome concentrates in spines upon KCl stimulation, which is due mainly to a decreased exit rate rather than an increased entry rate in spines. This proteasome sequestration after KCl treatment was speculated to be caused, to some degree, by the association between the proteasome and the actin cytoskeleton. Together, these results provide a mechanism by which the proteasome is recruited to spines in a NMDAR-dependent manner, where it is sequestered to locally remodel the PSD composition during KCl stimulation and maybe even beyond the stimulation period.

Neuronal activity regulates the synaptic composition through the proteasome [43], even so it does not imply that the proteasome itself could not be regulated. In fact, there is an increasing body of evidence [48], [49] that the proteasome may be modified by posttranslational modifications such as O-glycosylation and phosphorylation. Could those modifications be a consequence of neuronal activity and which are their implications in proteasome? To address some of these questions, Djakovic S. N. *et al* (2009) proved initially that TTX and bicuculline have antagonistic effects on proteasome activity in hippocampal neurons, i.e. the proteasome activity is adjusted according to the neuronal activity state. Moreover, these changes in proteasome activity were found to be mediated by $Ca^{2+}$ signaling, namely $Ca^{2+}$ influx through NMDAR and L-type voltage-gated calcium channels and subsequently by CaMKII, with CaMKII activation being

dependent on $Ca^{2+}$. This kinase phosphorylates *in vitro* Rpt6, a subunit of the 19S proteasome, but phosphorylation of Rpt6 *per se* appears to be insufficient to regulate proteasome activity *in vitro* [65]. So, a broader picture, taking in consideration other interactors to the proteasome, needs to be explored in order to understand ultimately how Rpt6 phosphorylation affects synaptic plasticity.

Following neuronal depolarization, both CaMKII and the proteasome translocate from dendritic shafts to spines, however their translocation occurs in an asynchronous manner, with CaMKII being translocated more rapidly than the proteasome [66],[67]. Given this temporal difference in CaMKII and proteasome dynamics, it was speculated that CaMKII could mediate the activity-dependent translocation of the proteasome to dendritic spines. In Bingol B. et al (2010), it was shown that CaMKII translocation, specifically αCaMKII autophosphorylated at Thr286, to spines is both necessary and sufficient to recruit the proteasome to the PSD, where αCaMKII is hypothesized to tether the proteasome stabilizing it. However, it remained unclear if the tethering of the proteasome in the PSD requires a physical interaction between CaMKII and the proteasome and if so, which proteasome subunit(s) are involved. The proteasome recruitment seems to be independent of CaMKII kinase activity toward heterologous substrates. Nevertheless, the phosphorylation of Rpt6 at Ser120 by CaMKII enhances proteasome activity [12]. Together, the evidence in this article gives insights about how CaMKII can modulate synaptic plasticity through the control of the proteasome recruitment and activity in the PSD, besides the phosphorylation of other synaptic proteins involved in learning and memory.

Later, further studies covering the functional relevance of Rpt6 phosphorylation to synaptic plasticity were carried out [68]. It was seen that Rpt6 is phosphorylated at Ser120 by CaMKII in an activity-dependent manner. Furthermore, this phosphorylation seems to be relevant for the sequestration of the proteasome in dendritic spines, which does not exclude that other phosphorylated residues of the proteasome might be involved. In terms of neuronal function, this article provides evidence that a single phosphorylation, at Ser120 of the Rpt6 subunit, modulates synaptic strength bidirectionally. This is proved by the differences in mEPSC amplitude, which increases or decreases in hippocampal neurons expressing a phospho-dead or a phospho-mimetic mutant of Rpt6 subunit, respectively. Interestingly, altered phosphorylation status both mimicked and occluded TTX and bicuculline chronic treatment, which seems to indicate that Rpt6 phosphorylation at Ser120 has a key role in homeostatic synaptic plasticity.

It is known for some time now that the GluN2B subunit binds to CaMKII [50]. A recent study by She K. *et al* (2012) found that in GluN2B (-/-) hippocampal neurons αCaMKII is unable to accumulate at synapses upon NMDAR activation, indicating that the GluN2A subunit cannot compensate for the lack of GluN2B in this respect. The specific effect of GluN2B in respect to CaMKII is based on a unique feature of the GluN2B C-terminus tail, the high affinity CaMKII binding site located on residues 1290 to 1309.

By now, we know that αCaMKII, after being activated and concentrated in dendritic spines, binds to the C-terminus of the GluN2B subunit. At the same time, activated αCaMKII mediates the recruitment of proteasome from dendritic shafts to spines, where αCaMKII, bond to GluN2B, acts as a scaffold to newly translocated proteasome sequestering it, in combination with actin, in spines. From the many targets of CaMKII as a kinase, the proteasome subunit Rpt6 seems to be one of them, whose phosphorylation not only seems to regulate the sequestration of the proteasome in spines but also influences its proteolytic activity. The latter seems to have a major role in the synapse, since it is through proteasome-mediated degradation, at least in part, that the neuronal proteome is degraded adjusting rapidly and efficiently the PSD content in response to neuronal activity. Despite the major advances in the field, some issues need to be clarified, such as 1) if GluN2B-containing NMDAR contribute to the sequestering of proteasomes in spines, 2) which specific protein(s) are degraded postsynaptically via the proteasome with relevance to synaptic function and also 3) whether the misregulation of proteasome distribution and function correlates with the pathogenesis of neurodegenerative and/or neuropsychiatric diseases, in which synaptic dysfunction is implicated.

## 2. OBJECTIVES

The proteasome is a ubiquitous complex with proteinase catalytic activity that, in the hippocampal glutamatergic neurons context, has a role in the local PSD remodeling intrinsic to normal synapse function. However, what are the molecular mechanisms behind the proteasome translocation from dendritic shafts to spines upon synaptic activity? Bingol B. *et al* (2010) and She K. *et al* (2012) shed light on these matters by connecting, respectively, the CaMKII to the proteasome and the CaMKII to the GluN2B subunit of NMDAR. Together, these articles prove that upon synaptic activity the recruitment and sequestration of the proteasome into PSDs is dependent on CaMKII and the GluN2B subunit. Nevertheless, a direct cause-effect between the GluN2B subunit and the proteasome was never studied.

A previous study carried out in our laboratory led to the observation that several proteasome subunits, namely α1, 3 and 6 and β1 and 2 subunits of the 20S proteasome, are decreased in PSDs of GluN2B(-/-) cortical neurons, when compared to WT ones [69]. This evidence raises the possibility that the GluN2B subunit might regulate the synaptic content of the proteasome under basal neuronal activity. Moreover, we speculated that the GluN2B subunit control over the proteasome could be beyond the regulation of proteasome content, for instance extended to the proteasome activity or even the proteasome mobility in and out of dendritic spines.

The mentioned hypotheses of proteasome regulation by the GluN2B subunit will be addressed in the following ways:

1) Through quantitative proteomic analysis, we found a lower content of the synaptic proteasome in GluN2B(-/-) PSD than wild-type ones. Thus, the first aim of this study is to confirm this previous observation through complementary approaches, such as assessing by quantitative immunocytochemistry the proteasome expression, either endogenous or overexpressed, at synapses of low density hippocampal cultures from GluN2B(-/-) and wild-type mice.

2) The proteasome activity is another aspect which could be regulated by the GluN2B subunit. Therefore, proteasome-dependent proteolysis will be assessed *in vitro* and in live neurons. Taking advantage of fluorogenic substrates or proteasomal degradation reporters in synaptoneurosomal fractions or low density hippocampal cultures, respectively, differences in proteasome activity dependent on the GluN2B subunit will be assessed.

3) Given the fact that the proteasome redistributes from dendritic shafts to spines in an activity-dependent manner and it is sequestered in synapses, even beyond postsynaptic depolarization [66], we will test, through the microscopy technique Fluorescence recovery after photobleaching (FRAP), the hypothesis that the GluN2B subunit might be involved in the mobility of proteasome in and out of dendritic spines in spontaneous activity conditions. .

4) Lastly, we will characterize the synaptic distribution of NMDA receptors and the proteasome throughout development in cultured hippocampal neurons, to understand whether it is possible that their synaptic localization is interdependent.

Overall, this project will contribute to understanding better how the proteasome is regulated by the GluN2B subunit, particularly at which level(s), in glutamatergic synapses under basal synaptic activity.

# 3. MATERIALS AND METHODS

## 3.1. MURINE MODELS

For primary neuronal cultures, hippocampi and cortices from 18 days-old embryos were used. For preliminary studies Wistar rat embryos were utilized, whereas in the cases where we addressed the relevance of the GluN2B subunit of NMDAR on proteasome regulation, genetically modified mice embryos (GluN2B(-/-) and wild-type littermates) were used. These genetically modified mice are the result of a targeted disruption of the mouse GluN2B subunit of NMDAR gene, which was interrupted by a neomycin-resistant gene, followed by its incorporation into the C57BL/6 mice genome [70].

Since the GluN2B subunit is vital for development [70], which translates in GluN2B knockout (GluN2B(-/-)) pups death after birth, the colony is maintained in heterozygosity. Therefore, embryos and pups (resulting from GluN2B(+/-) matings) have to be genotyped after dissection and birth, respectively.

## 3.2. PRIMARY CELL CULTURE

Pregnant females on embryonic day 18 (E18) were anaesthetized by 2-bromo-2-chloro-1,1,1-trifluoroethane (Sigma Aldrich®) and euthanized by cervical dislocation, according to the Directives from European Union on the protection of animals used for scientific purposes. Once embryos were removed, hippocampi and cortices were dissected and hibernated at 4ºC overnight in Hibernate E (BrainBits®) supplemented with NeuroCult® SM1 (Stemcell™ Technologies) until their genotypes were determined.

### 3.2.1. Culture genotyping

Genotyping of embryos was based on an established protocol [71], which uses polymerase chain reaction (PCR) amplification of genomic DNA as the procedure to get the genotypes. Succinctly, tails and brainstems were digested with 0.1mg/mL Proteinase K (Invitrogen™) at 55ºC for approximately 2h. After this, DNA was sequentially extracted using phenol/chloroform/isoamyl alcohol 25:24:1, precipitated with isopropanol, washed in ice cold 70% ethanol and resuspended in sterile water.

The genomic DNA was then amplified by PCR using a specific set of primers, sense and antisense, designed to address the GluN2B gene and the neomycin cassette, which

amplify the wild-type (WT) and mutant bands, respectively. Their nucleotide sequences are as follows:

| | |
|---|---|
| GluN2B | Sense 5' ATG AAG CCC AGC GCA GAG TG 3'<br>Antisense 5' AGG ACT CAT CCT TAT CTG CCA TTA TCA TAG 3' |
| Neomycin cassette | Sense 5' GGC TAC CTG CCC ATT CGA CCA CCA AGC GAA AC 3'<br>Antisense 5' AGG ACT CAT CCT TAT CTG CCA TTA TCA TAG 3' |

The amplification occurs according to the cycling conditions described in table 1. The 793 and 422 base pair fragments, PCR reaction products corresponding to amplified mutant and WT bands, respectively, were run in an 1% agarose gel, with the DNA fragments being visualized by SYBR® Safe fluorescence when it was exposed to ultraviolet (UV) light.

**Table 1.** Cycling conditions used in the PCR reaction.

| | **DNA denaturation** | | **Primers annealing** | **Primers extension** | **Final extension** |
|---|---|---|---|---|---|
| **# cycles** | 1 | 35 | | | 1 |
| **T / ºC** | 95 | 94 | 67 | 72 | 72 |
| **t /min** | 4 | 0.5 | 0.7 | 0.8 | 7 |

### 3.2.2. Cell culture

Once the genotypes were determined, the dissociation of hippocampi and cortices took place. The dissociation was characterized by two moments: these tissues are submitted firstly to an enzymatic dissociation by papain (20 units/ mL) and deoxyribonuclease (DNase) I (0.20 mg/ mL) at 37ºC for 10 min, and secondly to a mechanic dissociation which leads to a cellular suspension. Between those two moments, cells were washed with inactivation solution containing bovine serum albumin (BSA) and trypsin inhibitor to stop the enzymatic activity of papain and washed with $Ca^{2+}$- and $Mg^{2+}$-free Hank's balanced salt solution (HBSS: 5.36mM KCl, 0.44mM $KH_2PO_4$, 137mM NaCl, 4.16mM $NaHCO_3$, 0.34mM $Na_2HPO_4.2H_2O$, 5mM glucose, 1mM sodium pyruvate, 10mM HEPES and 0.001% phenol red) to clear BSA, avoiding the overgrowth of glia cells. Finally, the cellular suspension was plated in neuronal plating medium

(minimum essential medium (MEM) supplemented with 10% horse serum, 0.6% glucose and 1mM pyruvic acid) either onto poly-D-lysine-coated (0.1mg/mL) coverslips in 60mm culture dishes or in 6-well plates depending on the required type of culture, low or high density cultures, respectively. For low density cultures, hippocampal neurons were plated at a density of 350,000 cells *per* dish, while in the case of high density cultures, cortical neurons were plated at a density of 850,000 cells *per* well. After roughly 4 h in plating media, cells were attached to the extracellular matrix substrate and either the medium was changed to neurobasal medium supplemented with 2% NeuroCult® SM1, 0.5mM glutamine, 0.125µg/µL gentamicin and insulin (20µg/mL), in the case of high density cultures, or relatively to low density cultures, the coverslips were flipped over an astroglial feeder monolayer in supplemented neurobasal medium (with the same composition as described above). To restrain glial proliferation, at days *in vitro* (DIV) 3, 5µM cytosine arabinoside was added. Cultures were kept at 37ºC in a humidified incubator of 5% CO2/ 95% air, for a maximum of DIV 32.

Rat hippocampal cultures were prepared using the same procedure [56],[57] as mice cultures, with the exception of the enzymatic dissociation step, which was made in 0.25% trypsin for 15min at 37ºC.

### 3.3. PROTEIN EXTRACTS

Total extracts were prepared from DIV 16 cortical neurons, which had been transfected at DIV 13 with the Ub-G76V-GFP degradation reporter by the calcium phosphate method (see below). Neurons were washed once with ice-cold phosphate buffered saline (PBS: 137mM NaCl, 2.7mM KCl, 10mM $Na_2HPO_4$, 1.8mM $KH_2PO_4$, pH 7.4) before cells were lysed with ice-cold RIPA buffer (150mM NaCl, 50mM Tris-HCl (pH 7.4), 5mM EGTA, 1% Triton, 0.5% Deoxycholate (DOC) and 0.1% SDS) supplemented with a cocktail of protease inhibitors (0.2mM PMSF, 1µg/mL chymostatin, 1µg/mL leupeptin, 1µg/mL antipain, 1µg/mL pepstatin). The obtained lysates were sonicated on ice with an ultrasonic probe for 30s (6 pulses of 5s each alternated by 5s). After sonication, the samples were centrifuged at 16000g for 10min at 4ºC and the protein content of the supernatant, correspondent to soluble proteins, was quantified using the Bicinchoninic acid assay (BCA) method.

Membrane extracts were prepared according to an established protocol[74], which is similar to the one described above. Cells with DIV 14-15 were washed twice with ice-cold PBS and then once with PBS supplemented with a cocktail of protease inhibitors

(0.2mM PMSF, 1µg/mL chymostatin, 1µg/mL leupeptin, 1µg/mL antipain, 1µg/mL pepstatin). Cells were then lysed in lysis buffer containing 50mM Tris-HCl, pH 7.4; 5mM EGTA, 1mM DTT and supplemented with the previously mentioned cocktail of protease inhibitors plus the phosphatase inhibitors, 0.1mM sodium orthovanadate ($Na_3VO_4$) and 50mM sodium fluoride (NaF). The lysates were centrifuged at 16000g for 30min at 4ºC, the supernatant was discarded and the pellet was denatured with 2x denaturing buffer (250mM Tris, pH 6.8; 4% SDS; 200mM DTT; 20% glycerol and 0.01% bromophenol blue) at 95ºC for 5min.

### 3.4. SDS-PAGE, WESTERN BLOTTING AND QUANTIFICATION

Denatured extracts (50µg of total extracts or the whole volume of membrane extracts) were resolved by SDS-PAGE in Tris-glycine-SDS (TGS) buffer (25mM Tris, 192mM glycine, 0.1% SDS, pH 8.3) in 10% polyacrilamide gels 1.5mm thick at 60-80V. This was followed by overnight electrotransfer onto PVDF membranes, at 40V and 4ºC in transfer buffer (10mM CAPS pH 11, 10% methanol), complemented by a pulse of 1h at 100V in the morning. Membranes were then blocked for 1h at room temperature with 5% (w/v) skim milk (Regilait®) in TBT-T (Tris-buffered saline (TBS: 20mM Tris, 137mM NaCl, pH 7.6) with 0.1% Tween 20). Once blocked, the membranes were probed during 1h at room temperature or overnight at 4ºC with the correspondent primary antibody, anti-Rpt6 (Enzo®Life Sciences, raised in mouse) 1:1500 diluted in 1% (w/v) milk in TBS-T for membrane extract membranes and anti-GFP (Roche, raised in mouse) 1:1000 diluted in 0.5% (w/v) milk in TBS-T for total extracts. Following five washes in 0.5% (w/v) milk in TBS-T, the membranes were incubated for 1h at room temperature with alkaline phosphatase-conjugated secondary antibody, anti-mouse (Jackson ImmunoResearch Laboratories, Inc) 1:20000 diluted in 1% (w/v) milk in TBS-T or anti-mouse 1:20000 diluted in 5% (w/v) milk in TBS-T. After five washes in 0.5% (w/v) milk in TBS-T membranes were incubated with enhanced chemifluorescence (ECF) substrate and the fluorescence signal was detected on Storm 860 scanner (Amersham Biosciences).

As loading control, transferrin receptor was used, so striping and re-probing were needed. Firstly, ECF was removed by incubation in 40% methanol for 30min and then the membranes were washed in water (5 to 10 min) and incubated with NaOH 0.2M for 15min at room temperature. Membranes were again washed in water and blocked in 5% (w/v) milk in TBS-T for 1h at room temperature. Membranes were probed sequentially

with anti-human transferrin receptor antibody (Invitrogen™, raised in mouse) 1:1000 diluted in 5% (w/v) milk in TBS-T for 1h at room temperature and with anti-mouse antibody (Jackson ImmunoResearch Laboratories, Inc) 1:20000 diluted in 5% (w/v) milk in TBS-T. Next, the membrane was developed as previously described.

Band intensities, corresponding to the proteins under study, were quantified using ImageJ 1.45S software and normalized for the loading control, the transferrin receptor. The graphs present the GluN2B (+/+) versus the GluN2B (-/-) condition, with GluN2B(-/-) results being normalized against the control, GluN2B (+/+). The statistical analysis was made using Graph Pad Prism 5 software using paired t test.

### 3.5. SYNAPTONEUROSOMES

#### 3.5.1. Preparation

To obtain a considerable amount of the fraction of resealed pre- and postsynaptic elements, known as synaptoneurosomes (SNS)-rich fraction, 35 to $40x10^6$ cortical neurons, which is equivalent to approximately 47 wells (35 mm diameter) of a high-density culture of cortical neurons at DIV 15-16, were used.

SNS isolation was based on a previously reported protocol [75] with slight adaptations. Briefly, cortical neurons were washed with ice-cold HEPES-buffered sucrose (0.32M sucrose, 4mM HEPES, pH 7.4) and then collected with the same buffer used for washes, now supplemented with a cocktail of protease (0.2mM PMSF, 1µg/mL chymostatin, 1µg/mL leupeptin, 1µg/mL antipain, 1µg/mL pepstatin) and phosphatase (0.1mM $Na_3VO_4$ and 50mM NaF) inhibitors. The collected cells were submitted on ice to serial homogenizations, with a large clearance and next with a small clearance Teflon pestle in a Potter-Elvehjem homogenizer, each of 30 strokes. HEPES-buffered sucrose was added up to 8mL and 100µL of this homogenate was collected, which is considered the starting homogenate. The homogenate proceeded to centrifugation at 900g for 3min at 4ºC and the resulting supernatant was passed through 150 and 50 µm nylon filters, followed by a 5µm pore filter. The filtrate was then centrifuged at 10000g for 15min at 4ºC and the obtained pellet, enriched in SNS, was resuspended in 500µl of a buffer composed of 8mM KCl, 3mM $CaCl_2$, 5mM $Na_2HPO_4$, 2mM $MgCl_2$, 33mM Tris, 72mM NaCl, 100mM sucrose, pH 7.4.

The protein content of both the homogenate and the SNS fraction was quantified by the BCA method.

### 3.5.2. Validation of synaptoneurosome isolation

The SNS isolation was validated by WB analysis of subcellular markers, such as PSD-95, lamin A, synaptophysin, in the starting material and SNS fraction.

For WB analysis (performed as described above), 80µg of protein denatured in 5x denaturing solution were resolved on a 10% polyacrylamide gel, blotted and probed with the following primary antibodies [anti-PSD-95 1:2000 diluted in 0.5% milk in TBS-T (Cell Signalling Technology®, raised in rabbit), anti-lamin 1:1000 diluted in 0.5% milk in TBS-T (Sigma-Aldrich™, raised in rabbit), anti-synaptophysin 1:20000 diluted in 5% milk in TBS-T (raised in rabbit), anti-β actin 1:5000 diluted in 0.5% milk in TBS-T (raised in mouse)] followed by alkaline phosphatase-conjugated secondary antibody, anti-rabbit 1:20000 (Jackson ImmunoResearch Laboratories, Inc) or anti-mouse 1:20000 diluted in 5% (w/v) milk in TBS-T, depending on primary antibody host-species. The immunoreactivity was revealed using ECF and band intensities were quantified using ImageJ 1.45s and normalized for the loading control, β-actin.

### 3.5.3. Proteasome activity assay

The proteasome activity was assessed in both the homogenate and SNS fraction by an assay previously reported in the literature [76]. Succinctly, after the samples were collected, they were centrifuged at 16000g for 30s and the pellet was resuspended in 1mM EDTA; 10mM Tris-HCl, pH 7.5; 20% glycerol; 4mM DTT and 2mM ATP. Once the protein content was determined by the Bio-Rad Protein assay, the protein concentration in all samples was equalized.

The catalytic activity of the proteasome was estimated by the proteolytic activity of one of the 20S proteasomal β subunits, the β5 subunit with chymotrypin-like specificity, by monitoring the production of 7-amino-4-methylcoumarin (AMC) from the fluorogenic substrate suc-LLVY-AMC. To accomplish that, 20µg of each sample was incubated with 25µM suc-LLVY-AMC in the proteasome activity buffer (0.5mM EDTA; 50mM Tris-HCl pH 8.0; 2mM ATP), in a final volume of 100µL. The release of fluorescent AMC was measured at 37 °C using a microplate reader SPECTRAmax Gemini EM (Molecular Devices) at an excitation wavelength of 360 nm and an emission wavelength of 460 nm, for 60 min, at 5 min intervals. The specific activity of the β5 subunit, and, by extrapolation, the proteasome activity, was given by the subtraction of the total activity

minus the activity measured when the proteasome activity was blocked with 10µM MG132 (Calbiochem).

### 3.6. CALCIUM PHOSPHATE TRANSFECTION

Exogenous DNA was introduced into primary cultures using the calcium phosphate coprecipitation method [77]. This protocol was performed in rat low density cultures for cotransfection of CIM5 and DsRed-Homer1c constructs and in mouse high density cultures for transfection of the Ub-G76V-GFP degradation reporter construct.

Plasmid DNA (3µg *per* coverslip for CIM5 and 2µg *per* coverslip for DsRed-Homer1c in the case of rat hippocampal cultures and 10µg *per* well for the degradation reporter in mouse cortical cultures) were diluted in TE pH 7.3 (1M Tris-HCl, 250mM EDTA) and mixed with 2.5M $CaCl_2$ pH 7.2 in 10mM HEPES. Then, the DNA/TE/$CaCl_2$ solution was added, drop-wise, to 10 mM HEPES-buffered saline solution (270 mM NaCl, 10 mM KCl, 1.4 mM $Na_2HPO_4$, 11 mM dextrose, 42 mM HEPES), pH 7.2. The DNA/ calcium phosphate precipitates were allowed to form for 30min, protected from light, at room temperature with vortexing every 5min to help the formation of fine particles of precipitates. In the meantime, the neurons are prepared to be transfected by exposing them to 10mM kynurenic acid (Sigma Aldrich®), which prevents the toxicity inherent to transfection, in neurobasal medium previously in contact to neurons, known as conditioned medium. Once the precipitates were formed, they were added drop-wise, evenly through the whole coverslip or well depending on the type of culture transfected, and incubated for 3h at 37ºC/ 5% $CO_2$. After this incubation, the precipitates were dissolved in acidic medium (2mM kynurenic acid in supplemented neurobasal medium used for culture, which composition is described in Material and Methods's subsection "Cell culture", acidified with HCl until the solution acquires a bright yellow color) for 15min at 37ºC / 5% $CO_2$. Finally, the cells were restored to their conditioned medium and the constructs were allowed to be expressed up to DIV 16. In the case of CIM5 construct, its expression level starts to be assessed at 4h post-transfection. Cells were transfected at DIV 7 for CIM5 and DsRed-Homer1c constructs and at DIV 13 for the degradation reporter.

### 3.7. IMMUNOCYTOCHEMISTRY AND QUANTIFICATION

Coverslips used for GluN1 subunit immunostaining were fixed at DIV 5, 9, 13, 17 and 32 in 100% methanol for 10min at -20ºC and permeabilized straight after fixation

with PBS with a drop of 25% Triton X-100. A set of coverslips containing neurons with the same ages were fixed in pre-warmed 4% paraformaldehyde/ 4% sucrose for 15min at room temperature. The coverslips from CIM5 and DsRed-Homer1c-transfected rat hippocampal cultures were fixed at 4hrs post-transfection (with the transfection occurring at DIV 7), DIV 8, 10, 14 and 16 in pre-warmed 4% paraformaldehyde/ 4% sucrose for 15min at room temperature. After rinsing twice in PBS, neurons were permeabilized with 0.25% Triton X-100 (in PBS) for 5min at room temperature. After permeabilization, all coverslips were washed once in PBS for 5min and incubated with 10% BSA (in PBS) for 1h at 37ºC to block non-specific antibody binding. The coverslips were then incubated with the primary antibodies (table 2) in 3% BSA for 2h at 37ºC or overnight at 4ºC, with the exception of coverslips for GluN1 subunit immunostaining which requires overnight incubation with mild shaking at room temperature. After six washes with PBS, of 2min duration each, to remove unbound antibodies, the coverslips were incubated with secondary antibodies (table 2), depending on primary antibody' s host species, in 3% BSA for 1hr at 37ºC. Coverslips were washed once again six times with PBS, mounted in Fluorescent Dako mounting medium and sealed with nail polish.

**Table 2.** Characteristics of primary and secondary antibodies used for immunocytochemistry

| | Antigen | Dilution | Host | Supplier | | Antibody | Dilution | Fluorochrome | Supplier |
|---|---|---|---|---|---|---|---|---|---|
| **Primary** | **GluN1** | 1:1500 | mouse | Invitrogen™ | **Secondary** | Anti-mouse | 1:500 | Alexa Fluor® 568 or 350 | Molecular Probes™ |
| | **Rpt3** | 1:700 | rabbit | Enzo® Life Sciences | | Anti-rabbit | 1:500 | Alexa Fluor® 488 | Molecular Probes™ |
| | **PSD-95** | 1:200 | mouse | Thermo Scientific | | Anti-guinea pig | 1:500 | Alexa Fluor® 647 | Molecular Probes™ |
| | **GFP** | 1:500 | rabbit | MBL International Corporation | | Anti-chicken | 1:200 | AMCA | Jackson ImmunoResearch Laboratories, Inc |
| | **VGLUT1** | 1:5000 | guinea pig | Millipore™ | | | | | |
| | **MAP2** | 1:5000 | chicken | Abcam | | | | | |
| | **tau** | 1:500 | mouse | Synaptic Systems | | | | | |

Image acquisition was performed in a Zeiss Axiovert 200M inverted microscope, equipped with an AxioCam HRm camera, with a 63X1.4 NA (numerical aperture) oil-

immersion objective using Zen 2011 software (Carl Zeiss). The exposure time for each channel was set for random and healthy neurons, identified empirically by Microtubule associated protein-2 (MAP2) labeling, and maintained throughout each experiment.

Rpt3, GluN1, PSD95 and VGLUT1 clusters were quantified with ImageJ 1.45S. In all experiments, ten neurons *per* condition were quantified, in which two to three dendrites, selected by their MAP2 labeling, were chosen and their length measured, usually not less than 100µm. The aforementioned clusters were analyzed in respect to cluster number, area and intensity for the selected region, after the images were thresholded to include protein clusters. Plus, the cluster intensity was corrected for the background intensity of each image and the results were shown *per* dendritic length.

### 3.8. PROTEASOME MOBILITY *IN VIVO* ASSESSMENT

#### 3.8.1. Sindbis virus production

The Sindbis virus expression system was used for expressing heterologous proteins, namely the fluorescent protein mApple and the fusion protein that comprises enhanced GFP (EGFP) and Rpt1, in primary neuronal cultures. This system exploits the Sindbis virus life cycle by taking advantage of the Sindbis subgenomic promoter under which control the gene of interest is transcribed at high level, leading to high levels of the recombinant protein(s). The protocol followed was the one from Invitrogen with minor alterations. Briefly, upon the ligation of the gene of interest which codifies EGFP-Rpt1 or mApple, in the pSinRep5 plasmid vector, the cloned construct was linearized with the restriction enzyme XhoI (Nzytech, Lda – Genes & enzymes) and then transcribed *in vitro* into capped and polyadenylated transcripts. These recombinant RNAs plus the DH(26S) RNA, helper RNA which provides the *in trans* structural proteins that make up the virus capsid, were electroporated into BHK (Baby Hamster Kidney) cells to produce fully packaged pseudovirions. After 24 to 36h post-transfection, the medium containing the pseudovirions was harvested and purified by ultracentrifugation at 22000 rpm during 2h20 at 15ºC. The resulting pellet was resuspended in PBS with 0.1% BSA and the optimal amount of virus to infect, for obtaining the higher protein expression with less neuronal death, was determined empirically through serial dilutions of the virus stock.

#### 3.8.2. Fluorescence Recovery after Photobleaching

Previously to the live cell assessment of proteasome dynamics through FRAP analysis, hippocampal neurons were co-transfected at DIV 7 with both CIM5 and DsRed-

Homer1C constructs and the neurons were let to express the proteins for 4 to 36 hrs post-transfection. Later on, as an approach for getting higher expression of Rpt1-EGFP protein hippocampal cultures were co-infected at DIV 13 with both EGFP-Rpt1 RNA and mApple RNA pseudovirions. Each coverslip to be infected was transferred to a multiwell with conditioned medium (with the neurons facing up) and the mentioned pseudovirions were added to the medium. After six hours of infection at 37ºC/ 5% $CO_2$, the medium was removed by suction, the coverslips were washed once with sterile PBS and then the coverslips were once again flipped over the glia feeder layer in their conditioned medium. The recombinant RNAs were let to be translated into the respective proteins for approximately 36h.

All the FRAP experiments were performed at room temperature with the Carl Zeiss LSM 510 Meta confocal microscope using a PlanApoChromat 63X1.4 NA oil-immersion objective. The coverslip to be observed was mounted on a pre-greased chamber for coverslips with a clear aperture diameter of10 mm and maintained in pre-heated (to 37ºC) HEPES-buffered solution (HBS) (110mM NaCl, 5.4mM KCl, 1.8mM $CaCl_2$, 0.8mM $MgCl_2$, 10mM D-glucose, 10mM HEPES-NaOH (pH 7.4)).

Initially the regions to be bleached would have been selected either through DsRed-Homer1C protein, which should label synapses, or mApple protein, which is expressed throughout the entire neuron. Given a limitation of the imaging chamber used combined with limitations in co-transfection and co-infection, the identification of bleaching ROI was made using the EGFP-Rpt1 signal. Once the dendritic spines were identified, a crop with a 2x zoom was made to zoom in on that dendrite. Next, a ROI was drawn around the spine to be monitored and the fluorescence corresponding to Rpt1-EGFP protein was bleached for 20 iterations using the laser at 80% intensity.

# 4. RESULTS AND DISCUSSION

## 4.1. THE GLUN2B SUBUNIT DOES NOT INFLUENCE THE PROTEASOME CONTENT IN CORTICAL NEURONS

Throughout the last years, it has been seen that the GluN2B subunit of NMDAR, through its interaction with CaMKII, has an essential role in PSD reorganization subjacent to glutamatergic transmission in the hippocampus. Among the so many remodeling events induced by neuronal activity, the dynamics of the proteasome in and out of dendritic spines is one of those events, with NMDAR containing the GluN2B subunit, and also CaMKII, regulating its localization. But how does GluN2B function as an anchor in PSDs translate in terms of proteasome content? Our laboratory found insights into this matter through quantitative proteome analysis of PSDs isolated from cortical neurons, where GluN2B absence seems to lead to a decrease in several proteasome subunits like 20S proteasome alpha subunits 1, 3, 6 and 7 or beta subunits 1 and 2 [69].

Aiming to seek additional confirmation of this observation, we assessed by western blotting (WB) the proteasome content in membrane extracts obtained from mice cortical neurons at DIV 14-15. Specifically, the Rpt6, an ATPase subunit of the 19S proteasome, was the one analyzed and no significant difference was seen between membrane extracts from GluN2B(+/+) and GluN2B(-/-) cortical neurons (Figure 5) in terms of normalized Rpt6 levels. At first glance the results from WB (Figure 5) seem to be contradictory when compared to the ones obtained from quantitative proteome analysis, where the

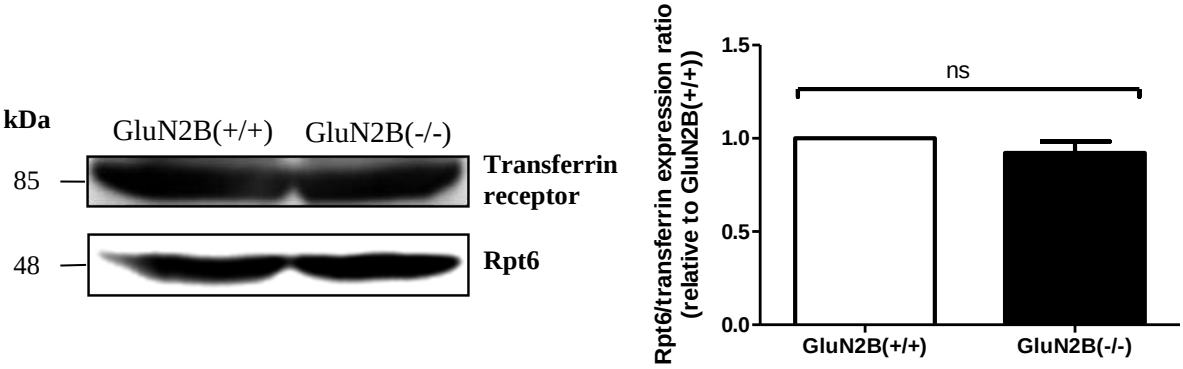


**Figure 5. The GluN2B subunit does not influence the expression of Rpt6 in total membrane extracts of mice cortical neurons.** Membrane protein extracts of mice cortical neurons were prepared at DIV 14-15 and assessed by WB for Rpt6, a 19S proteasome subunit, and for transferrin receptor, which is the loading control. The resultant probed WB membranes, as the one shown on the left in this figure, show a comparison of transferrin receptor and Rpt6 expression between wild-type (GluN2B(+/+)) and mutant (GluN2B(-/-)) extracts. On the right, the bar graph depicts the mean ratio between Rpt6 and transferrin receptor levels ± SEM relative to the ratio of these proteins in GluN2B(+/+) extracts. No significant difference in Rpt6 levels between GluN2B(+/+) and GluN2B(-/-) membrane extracts is seen. The statistical analysis is based on paired t test for five independent experiments.

proteasome levels, at least some α and β 20S proteasome subunits, are reduced in GluN2B(-/-) PSDs compared to PSDs isolated from wild-type neurons [69]. However, whereas the PSD fraction is a subcellular fraction containing mostly PSD-resident proteins, which are specific to postsynaptic excitatory compartments, whole membrane extracts contain total membrane proteins and their associated partners. In fact, the proteasome is also abundant in the cell body and at presynaptic sites [78]; therefore the results obtained with the membrane extracts reflect the whole cellular content in the proteasome, whereas the PSD data refers to the postsynaptic proteasome. It would be useful to analyze other proteasome subunits, since these two results analyzed different complexes of the 26S proteasome, the 20S proteasome in isolated PSDs and the 19S proteasome in membrane extracts.

Summing up, the two results are not directly comparable but, *per se* the results obtained from cortical membrane extracts can indicate that the whole cell proteasome content, with Rpt6 subunit as a representative of it, does not vary when GluN2B subunit is absent. However, the level of a subunit from 20S proteasome should have been assessed along with Rpt6 subunit because the 26S proteasome should not be taken as a whole by one of its complexes.

### 4.2. SYNAPTONEUROSOMES WERE SUCCESSFULLY PURIFIED FROM MICE CORTICAL NEURONS

Following up the last result, synaptoneurosomes were the subcellular neuronal fraction selected to continue the evaluation of proteasome expression in the absence of the GluN2B subunit of NMDAR. Synaptoneurosomes are made by sealed presynaptic sacs (synaptosome) attached to their corresponding resealed postsynaptic counterparts (neurosome) [79]. Since synaptoneurosomes retain pre- and postsynaptic characteristics, inclusively the molecular machinery necessary for neuronal transmission, this fraction is considered to contain physiologically active synapses [80]. Ideally, we should have used PSDs, since it is the only subcellular neuronal fraction that allows excluding the effect of presynaptic contribution on proteasome content. However, given the time necessary to purify PSDs, the synaptoneurosomes were selected over PSDs. Moreover, we expect the presynaptic proteasome contribution to be identical in GluN2B(+/+) and in GluN2B(-/-) neurons.

Isolated synaptoneurosomes should be enriched in synaptic proteins when compared to homogenates. On the contrary, somatic proteins should be absent or reduced in

synaptoneurosomes. In fact, biochemical characterization of synaptoneurosomes (Figure 6, panel A) shows what was expected, with synaptophysin, a presynaptic vesicle protein [81], and PSD-95, a hallmark of postsynaptic densities [82], being increased. Conversely, lamin A, an intermediate filament protein of nuclear lamina [83] which is restricted to the cell body, is reduced in synaptoneurosomes.

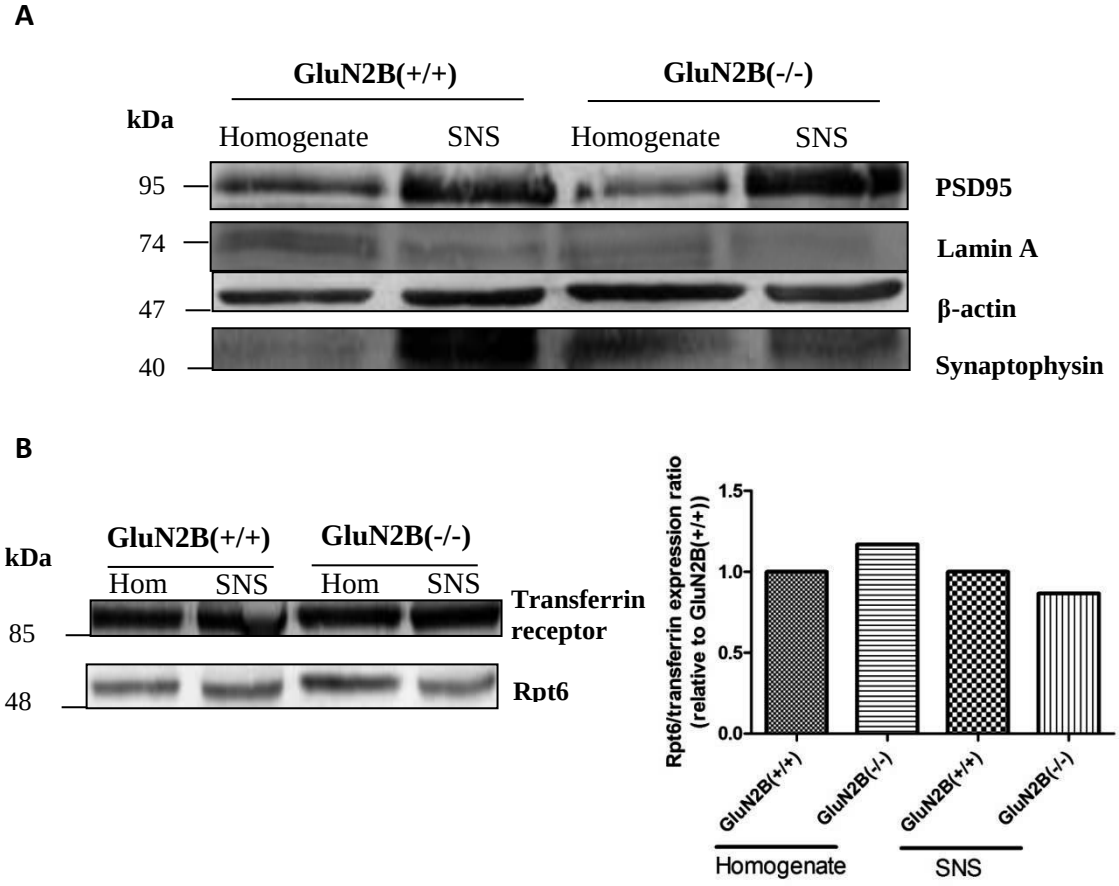


**Figure 6. Synaptoneurosomes were successfully purified from mice cortical neurons. No significant difference in Rpt6 expression between GluN2B(+/+) and GluN2B(-/-) homogenates (hom) or synaptoneurosomes (SNS) was found.** The SNS are prepared from homogenates of mice high density cortical neurons with 15-16DIV; purified SNS were validated biochemically assessing the expression of synaptic protein markers, as well as cell soma protein. An enrichment or reduction in the expression of these markers is expected depending of its localization, synaptic or somatic respectively. Panel **A** shows the validation of SNS purification through WB where it is seen that SNS are enriched in synaptic proteins, like presynaptic synaptophysin and postsynaptic PSD-95, when compared to homogenates. On the contrary, somatic proteins, such as lamin A, are less abundant in SNS. β- actin acts as the loading control. Panel **B** presents a WB and its corresponding bar graph translating the ratio between expression of Rpt6, a 19S proteasome subunit, and transmembranar receptor of transferrin for homogenates and SNS. No significant difference is seen when both genotypes within each cellular fraction (homogenate or SNS) are compared. Nevertheless, only 1 experiment was made, so repetition of this experiment is mandatory. In this case, the loading control was the transmembranar receptor transferrin.

At DIV 14-15, the synaptoneurosomes were isolated from homogenates of mice high density cortical neurons and the levels of Rpt6 subunit were assessed by WB for both genotypes in homogenates and synaptoneurosomes (Figure 6, panel B). Apparently, no

noticeable difference is seen between GluN2B(+/+) and GluN2B(-/-) genotypes for both homogenates and synaptoneurosomes in terms of normalized Rpt6 levels. Given the fact that only 1 experiment was made, the conclusions taken from these results are preliminary, however these results suggest that in synaptoneurosomes, containing both pre- and post-synaptic terminals, it is not possible to detect changes in the Rpt6 subunit levels in the absence of the GluN2B subunit.

### 4.3. THE LEVEL OF PROTEASOME IN AXON-LIKE NEURITES SEEMS TO BE LOWER THAN IN DENDRITE-LIKE NEURITES OF RAT HIPPOCAMPAL NEURONS TRANSFECTED WITH CIM5 CONSTRUCT

Attempting to find out if and to which extent the presynaptic site has a contribution on the whole cell proteasome content (Figure 5), we cotransfected at DIV 7 rat hippocampal neurons with a CIM5 construct, which comprises the Rpt1 subunit and GFP coding sequences, and DsRed-Homer1c construct, which will be translated into a fusion protein comprising the excitatory postsynaptic protein Homer1c and a red fluorescent protein DsRed. These constructs were expressed until DIV 16, after which the neurons were immunostained for GFP, tau and VGLUT1. Initially, our aim was to quantify the number of synaptic GFP-labeled puncta at DIV 16, i.e. the Rpt1 subunit of the proteasome, where synapses were to be defined by the colocalization of the presynaptic protein VGLUT1 and the postsynaptic protein Homer1c. However, the Homer1c expression at DIV 16 is not restricted to synapses (result not shown) and also some GFP puncta are impossible to tell apart with the overexpression of the Rpt1 subunit, making untrustworthy the puncta quantification. Therefore, we looked at the Rpt1 signal in a qualitative manner, trying to compare the abundance of the proteasome in dendrites and axons by comparing the tau-labeled axon-like neurites with dendrite-like ones, not labeled for tau. The distinction between axon- and dendrite-like neurites is based strictly on the cytoskeletal protein tau labeling, which is axonally compartmentalized in DIV 16 mature hippocampal cultures, and on morphological characteristics like: dendrite-like neurites are thicker than axon-like neurites and axon-like neurites tend to be crisscrossed and to surround dendrite-like ones forming ropelike fascicles [84], as shown in Figure 7. In fact, this characteristic makes it difficult to distinguish between the axonal and dendritic proteasomes, since dendrites are often surrounded by axons. To overcome this difficulty, we could immunostain dendrites for the cytoskeletal protein MAP2, dendrite-specific at DIV 16 [84], or even use confocal microscopy instead of fluorescence widefield

microscopy, aiming to obtain ultimately a Z-stack that allows to distinguish undoubtedly GFP-labeled proteasome subunit from axon- and dendrite-like neurites.

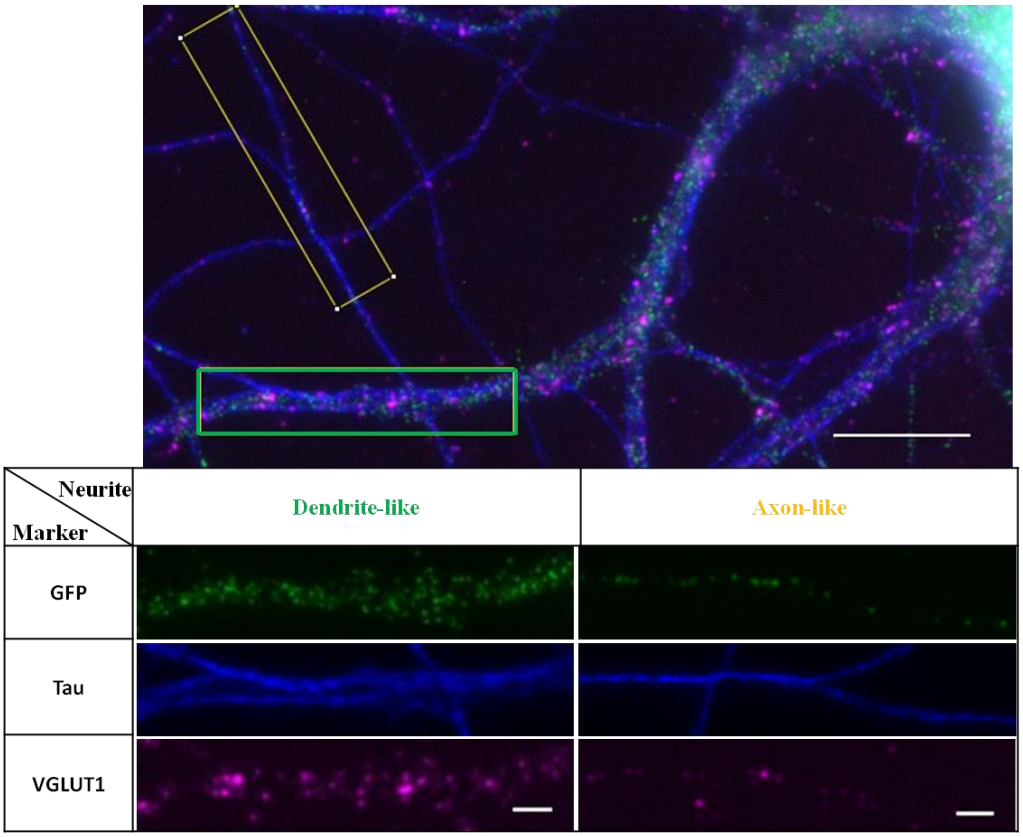


**Figure 7. The level of the proteasome in axon-like neurites is lower than in dendrite-like neurites of CIM5-overexpressed rat hippocampal neurons.** Low density rat hippocampal cultures were transfected with the CIM5 construct, which will be translated into a fusion protein combining the Rpt1 subunit of the proteasome with the GFP protein, at 7 DIV and this construct was expressed until 16 DIV, after which the neurons were fixed and immunostained for GFP, tau and VGLUT1, which labels, respectively, the transfected Rpt1 subunit, the axonal microtubule-associated protein and the vesicular glutamate transporter 1. The dendrite-like neurites (green rectangle) were strictly identified by being the thicker surrounded by fine-calibre neurites, the ones considered axon-like neurites (yellow rectangle) and presenting tau labeling, which could form ropelike fascicles around dendrite-like neurites. Qualitatively, the GFP-labeled proteasome subunit, Rpt1-GFP, seems to be less abundant in axon-like neurites than in dendrites-like neurites. Scale bar 10 µm; scale bar (crop) 2 µm

Nevertheless, facing this preliminary result (Figure 7), the contribution of the presynaptic proteasome on whole cell proteasome content (Figure 5) should be small, given that the GFP-Rpt1 subunit labeling is apparently more abundant in dendrite-like neurites when compared to axon-like neurites and given also the fact that this result is focusing on Rpt1 subunit overexpression.

### 4.4. THE GLUN2B SUBUNIT ABSENCE LEADS TO THE DECREASE OF PROTEASOME ACTIVITY *IN VITRO* AND *IN VIVO*

In addition to the proteasome content, other aspects of the proteasome could be affected in the absence of GluN2B, like for example the proteolytic activity of the 20S proteasome. This proteolytic activity is conferred by three β subunits, β1, 2 and 5, integrated within the 20S proteasome, each with its own specificity towards different N-terminal residues. To investigate the influence of the GluN2B subunit on the proteasome activity, we took advantage of the fluorogenic substrate suc-LLVY-AMC, which allows quantifying the free AMC fluorescence resultant of suc-LLVY-AMC cleavage by the β5 subunit. Since the β5 subunit, a N-terminal hydrolase with chymotrypsin-like specificity, is the one responsible for the rate-limiting step in protein hydrolysis [26], the proteasome activity is solely extrapolated from the activity of the β5 subunit. However, suc-LLVY-AMC hydrolysis could measure not only the proteolytic activity of the β5 subunit but also of other chymotrypsin-like peptidases, so we measured also the AMC fluorescence in the presence of the reversible 20S proteasome inhibitor, MG132. Thus, the specific proteasome activity is given by the total proteolytic activity, proteasome and non-proteasome dependent, subtracting the proteolytic activity when the proteasome is inhibited. The proteasome activity was quantified in mice cortical homogenates and purified synaptoneurosomes with DIV 15-16 in the presence of ATP. The specific proteasome activity is significantly decreased in GluN2B(-/-) homogenates when compared to wild-type ones (Figure 8A, left). However, no significant difference was found in the proteasome activity in synaptoneurosomes from both genotypes (Figure 8A, right), although, contrary to what was expected, the proteasome in GluN2B(-/-) synaptoneurosomes show a trend to be more proteolytically active than in GluN2B(+/+) synaptoneurosomes (Figure 8A, right). Several aspects should be taken in consideration in order to try explaining these controversial results. Firstly, the homogenates correspond to a fraction where the neurons were lysed, so by analyzing the proteasome activity *per se* we could be excluding proteasome interactors that exist in an *in vivo* system and could modulate proteasome activity. Nevertheless, the proteasome activity difference between GluN2B(+/+) and GluN2B(-/-) homogenates is undeniable, therefore the explanation for this could be on the proteasome itself rather than in its interactors, assuming that the interactions with the proteasome are disturbed with homogenization.

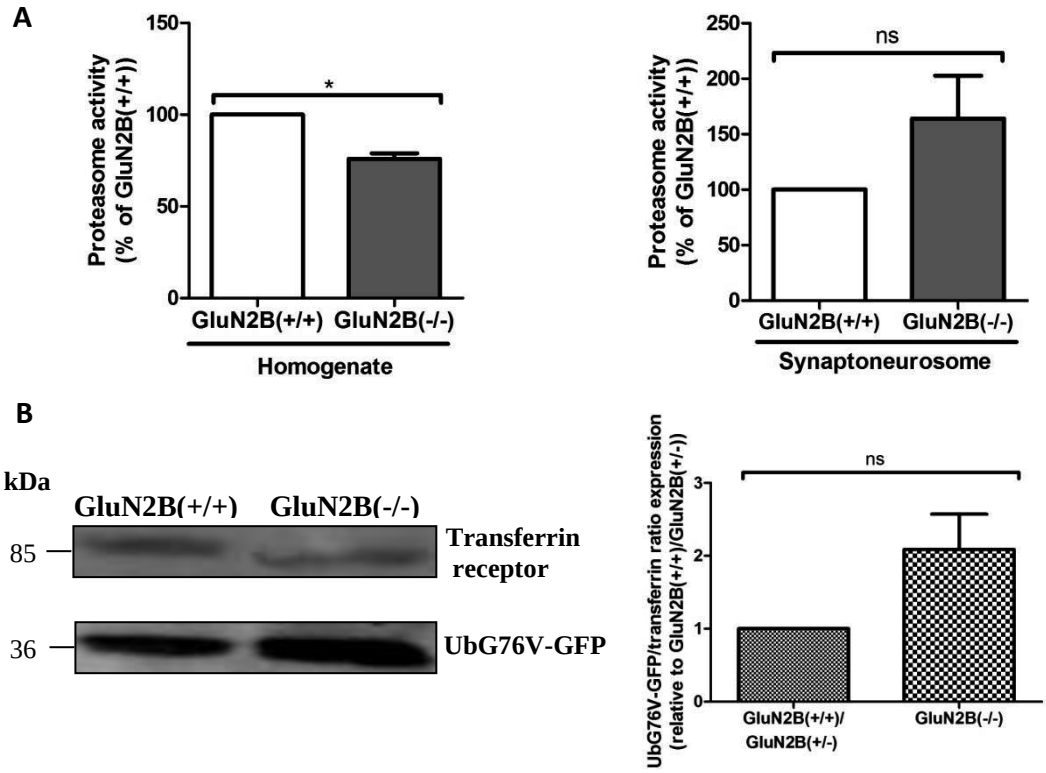


**Figure 8. The proteasome activity is diminished in the absence of the GluN2B subunit.** The ubiquitin/proteasome-mediated proteolytic activity was evaluated either by the hydrolysis of the fluorogenic substrate suc-LLVY-AMC in mice cortical homogenate and synaptoneurosome fractions (panel A) or by the assessment via WB of the GFP-based proteasomal degradation reporter ($Ub^{G76V}$-GFP) levels in mice cortical extracts (panel B). Proteasome activity is quantified through measuring the AMC fluorescence, hydrolysis product of fluorogenic substrates. In this case, the proteasome activity is extrapolated from the activity of β5 subunit of the 20S proteasome, subtracting the hydrolysis of suc-LLVY-AMC that is independent of the proteasome. Panel **A** shows thus the specific proteasome activity ± SEM. The proteasome activity in GluN2B(-/-) neuronal homogenates is significantly reduced when compared to GluN2B(+/+) ones. Interestingly, the proteosome activity in synaptoneurosomes is not in agreement with the results obtained from homogenates. In fact, GluN2B(-/-) synaptoneurosomes appear to have an increase in proteasome activity when compared to GluN2B(+/+) ones. The statistical analysis follows a paired t test for three independent experiments.

For quantification of proteasome activity in living cells, we transfected mice cortical neurons with $Ub^{G76V}$-GFP construct at 13 DIV and left them express this degradation reporter until 16 DIV. Panel **B** shows the resulting western blot, where the degradation reporter and the transferrin receptor were labeled, the latter serving as loading control. In the bar graph, as well as in the blot, it is visible a considerable increase in the levels of $Ub^{G76V}$-GFP in GluN2B(-/-) neuronal protein extracts in opposition to GluN2B(+/+)/ GluN2B(+/-) ones. This accumulation means that proteasome activity is decreased when the GluN2B subunit is absent. The statistical analysis is based on a paired t test for three independent experiments.

In additional experiments, we turned to a degradation reporter, namely the $Ub^{G76V}$-GFP, which can provide us more credible results about the ubiquitin-dependent proteolysis since we are evaluating the reporter turnover in live cells instead of performing an *in vitro* assay after cell lysis, such as when using the suc-LLVY-AMC assay. The degradation reporter $Ub^{G76V}$-GFP is a destabilized GFP variant, i.e. short-lived

variant, which combines N-terminally the GFP protein with a constitutively active ubiquitin fusion degradation (UFD) signal. This UFD signal is the acceptor for polyUb chains and consists of a mutated ubiquitin in the last aa that prevents the cleavage of this ubiquitin by deubiquitinating enzymes [85],[86]. To assess the proteasome activity in live neurons, mice cortical neurons were transfected at DIV 13 with the $Ub^{G76V}$-GFP construct and the construct was expressed until DIV 16, after which the neurons were lysed and analyzed via WB for GFP-based proteasomal degradation reporter and transferrin receptor levels. The accumulation of the degradation reporter translates a decreased proteolysis of this reporter by the proteasome. We assessed the $Ub^{G76V}$-GFP levels in wild-type and GluN2B(-/-) cortical neurons, and observed an accumulation of the degradation reporter in the absence of the GluN2B subunit (Figure 8, panel B). Although the difference is still not statistically significant, the levels of the degradation reporter are considerably increased in GluN2B(-/-) neurons when compared to wild-type/ GluN2B(+/-) ones. The individual results from GluN2B(+/+) and GluN2B(+/-) cultures were pooled together in this analysis since previous studies in our laboratory showed that the NMDAR synaptic content is unaltered in GluN2B(+/-) neurons compared to wild-type. While the fluorogenic substrate suc-LLVY-AMC can be degraded in the proteasome independently of ubiquitin tagging [87], the $Ub^{G76V}$-GFP reporter is dependent of ubiquitin for being degraded in the proteasome. So, the GluN2B subunit absence could affect the proteasome activity indirectly by interfering with an upstream step of proteasome like ubiquitination. However, given the concordance between the results (Figure 8, panel A and B) from suc-LLVY-AMC assay in homogenates and the degradation reporter in total extracts, it is plausible to say that the absence of GluN2B subunit decreases the proteasome activity, probably by interfering with this proteolytic complex rather than with the covalent conjugation of ubiquitin.

### 4.5. PROTEASOME MOBILITY ANALYSIS THROUGH FRAP – ATTEMPTS FOR IMPLEMENTING THIS TECHNIQUE

In 2006 Bingol B. and Schuman E.M. showed, through photobleaching techniques, that the immobile fraction of the Rpt1-EGFP fusion protein in stimulated neurons is considerably bigger than its immobile fraction in basal conditions, which means that neuronal activity increases proteasome sequestering in spines. This proteasome sequestration was attributed in part to the association to actin cytoskeleton. In 2010, Bingol B. *et al* brought new light to this issue by reporting that αCaMKII translocates to

spines, where it tethers the proteasome, in a NMDAR activity-dependent manner. Therefore, given these studies and the fact that CaMKII, once activated, binds to GluN2B subunit [50], it is worth exploring if GluN2B subunit could be implicated on proteasome mobility.

To explore how proteasome mobility in spines is affected by the GluN2B subunit, we designed co-transfecting GluN2B(+/+) and GluN2B(-/-) hippocampal neurons with Rpt1-EGFP construct together with DsRed-Homer1C one. After letting the constructs be expressed, fluorescence recovery after photobleaching (FRAP) imaging would allow seeing how the fluorescence of the fluorescent-tagged Rpt1-EGFP recovers after being bleached. DsRed-Homer1C construct would allow us to localize spines and consequently select the region where it would be done the photobleaching for Rpt1-EGFP signal. This was the initial plan, but some limitations restricted how far FRAP was implemented. The major limitation was that the yield of co-transfection was low; therefore spines and, by extension, the region of interest (ROI) for bleaching was defined by Rpt1-EGFP signal rather than by the DsRed-Homer1C signal. Moreover, the Rpt1-EGFP fluorescence was low for live cell imaging, even if it colocalized to endogenous Rpt1 (data not shown). Nevertheless, even on a low-level expression range, empirically it was seen that the highest expression for Rpt1-EGFP protein was for 36 hrs after transfection at DIV 7 of rat hippocampal neurons.

In order to increase Rpt1-EGFP expression and, by extension, fluorescence to levels appropriate to FRAP experiments we tried co-infecting hippocampal neurons with both mApple and Rpt1-EGFP RNA pseudovirions. Since mApple protein is expressed throughout the whole neuron, this protein would have been helpful identifying the structures projecting from dendrites, i.e. the spines. This approach via infection turns out to be extremely toxic to neurons, in particular to GluN2B (-/-) hippocampal neurons, which are by nature feeble and sensitive. Like in transfection, the rate of infection occurs with higher probability towards coverslip edges. This area was lost when the coverslips were mounted in the imaging chamber for FRAP.

Nevertheless, we made some attempts at implementing FRAP imaging of Rpt1-EGFP. Time-lapse imaging of the fluorescence signal for Rpt1-EGFP was performed at single spines in rat hippocampal neurons 36 hrs post-transfection, before and after photobleaching. (Figure 9A). The fluorescence intensity of Rpt1-EGFP fusion protein was quantified in three regions of interest (ROI)s for all time-frames obtained during the FRAP experiment. These ROIs were defined to the following regions: 1) bleaching,

represented by a blue circumference in Figure 9A, where protein mobility is assessed; 2) outside of the neuron, addressing the background fluorescence and 3) region in the neighboring dendrite to the spine bleached, accounting for fluctuations in laser intensity and acquisition photobleaching. Therefore, the fluorescence intensity must be background-subtracted, corrected and then normalized. Then, the normalized fluorescence of Rpt1-EGFP protein in bleached region could be plotted over time (Figure 9B). Since the plot is constructed out of only one FRAP experiment and there is some clear oscillations in the fluorescence along time, apart from around photobleaching (4,98 s), the parameters which could be extracted from a FRAP recovery curve will be exemplified based on an idealized FRAP recovery curve (Figure 9C). The recovery of fluorescence in the bleached area gives information about the molecules of the protein under study that were sequestered in the bleached region (the immobile fraction ($F_i$)), those that move into the bleached region (the mobile fraction ($F_m$)) and also the time that takes for recovering half the fluorescence of this protein in the bleached region after photobleaching ($t_{half}$). Since protein mobility is a relative concept in time, these parameters are only valid for the time-course of the experiment.

Even though we could not test if and how the GluN2B subunit influences the fluorescence recovery of Rpt1-EGFP protein, we made some progress on that direction and saw that, in a basal condition, the fluorescence intensity of Rpt1-EGFP increases after bleaching which could mean that Rpt1-EGFP moves into the bleached area. Nevertheless, further experiments need to be made, after sorting some technical aspects about FRAP like the chamber for imaging and the control of both temperature and $CO_2$.

**A**

**Before bleaching (4s)**

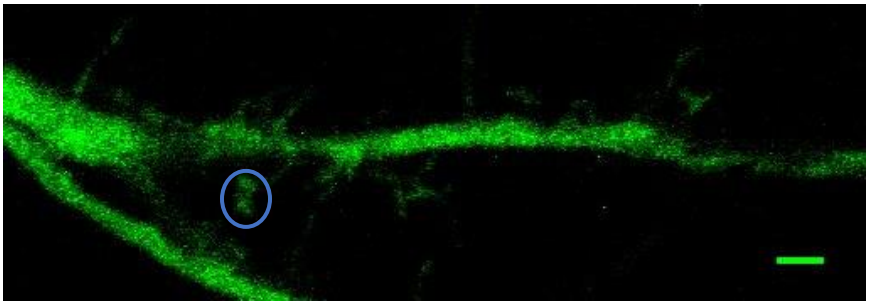

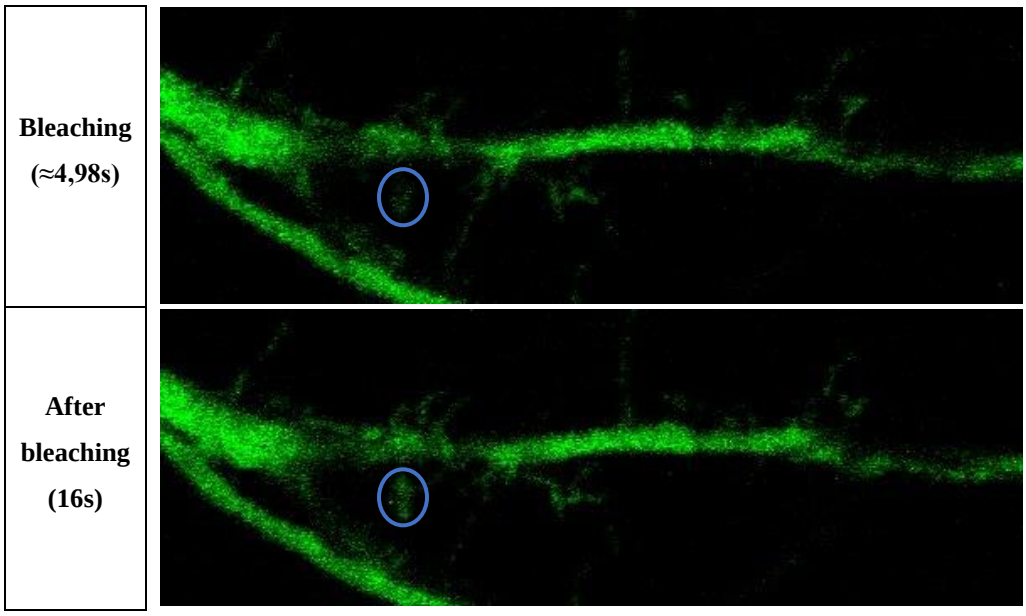


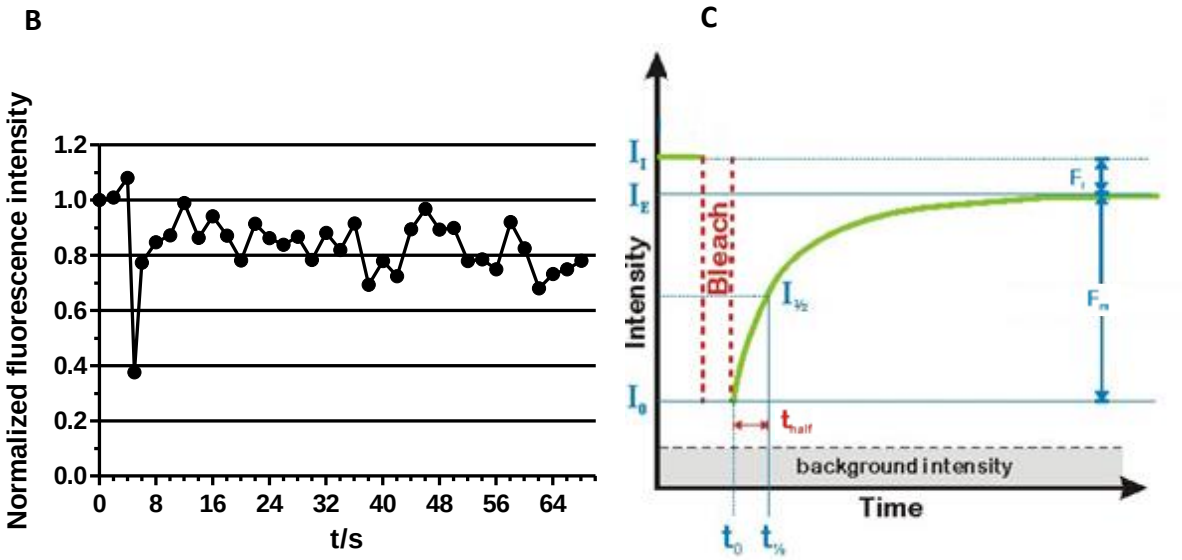


**Figure 9. Fluorescence recovery after photobleaching (FRAP) of Rpt1-EGFP in a spine of hippocampal rat neurons, and analysis of protein mobility parameters taken out of FRAP recovery curves. (A)** Rat hippocampal cultures were transfected with the CIM5 construct encoding Rpt1-EGFP at DIV 7. After letting the fusion protein comprising Rpt1 subunit and GFP protein be expressed for 36hrs, FRAP experiments were done. In this example, FRAP for the fusion protein was done in spines. The region of interest (ROI) for bleaching, where it was assessed if protein mobility occurs, was the one defined as a blue circumference in **(A)**. Even without the fluorescence intensity being corrected and normalized, it is possible to see that the fluorescence intensity of the fusion protein under study decreases at bleaching, when compared to a moment, approximately 1s, before bleaching. Furthermore, the fluorescence intensity increases after bleaching, which could be attributed to the mobility of Rpt1-GFP fusion protein into the bleached region. So, in the time-frame of the FRAP experiment Rpt1-EGFP fusion protein was mobile. Scale bar 2 µm. **(B)** shows a plot of normalized fluorescence intensity versus time (t). **(C)** depicts an idealized FRAP recovery curve from which certain parameters could be extracted like: mobile fraction ($F_m$); immobile fraction ($F_i$) and half-time of recovery ($t_{half}$), which are only valid for the time-course of the FRAP experiment. Plot **(C)** retrieved from www.embl.de/eamnet/frap/html/halftime.html.

### 4.6. THE GLUN1 SUBUNIT AND RPT3 SUBUNIT EXHIBIT SIMILAR PATTERNS OF EXPRESSION DURING HIPPOCAMPAL CULTURE DEVELOPMENT

Back in 1998, Rao A. and colleagues observed, through qualitative analysis of PSD-95 and NMDAR clustering during glutamatergic postsynaptic sites formation and development in cultured hippocampal neurons, that PSD-95 is not sufficient to recruit NMDAR to dendritic spines. Nevertheless, when NMDAR become synaptic, they are always located nearby PSD-95, consistent with the organizer role of PSD-95 in postsynaptic densities, and with the fact that NMDAR interact with PSD-95 via the GluN2B subunit [5]. So, back then it was unclear which were the molecular executors required for the synaptic localization of NMDAR. Being NMDAR and the proteasome two of the elements essential for glutamatergic synapse function, we followed the spatial distribution of NMDAR and the proteasome during the development of excitatory postsynaptic sites in cultured hippocampal neurons. The colocalization of the proteasome Rpt3 subunit with GluN1 subunit of NMDAR or PSD-95 was assessed during the development of low density rat hippocampal cultures at specific time points, namely DIV 5, 9, 13, 17 and 32, by immunocytochemistry followed by colocalization quantification. Moreover, the synaptic localization of Rpt3 subunit, GluN1 subunit and PSD-95 puncta were also quantified at the abovementioned developmental stages, by determining the colocalization of these proteins with the presynaptic marker VGLUT1. The DIV 5 time point was chosen as it corresponds to the approximate time when axodendritic contacts begin to happen. The colocalization of PSD-95 with the Rpt3 subunit or even its synaptic localization was also taken in consideration.

While the colocalization between Rtp3 subunit and the GluN1 subunit, the obligatory subunit of NMDAR, increases throughout development, with the exception of DIV 32, the colocalization between Rpt3 subunit and PSD-95 fluctuates (Figure 10, panels A and B). This is verified for all aspects of the puncta colocalization quantification, namely number, area and intensity. Despite the limits of resolution in optical microscopy and even the limitations of widefield fluorescence microscopy in terms of out-of-focus light that offer little guarantee for the spatial colocalization of the Rpt3 subunit and GluN1 subunit, these results suggest that these two subunits could be in close proximity to each other and be involved in their mutual localization along the development of cultured hippocampal neurons. The interesting observation that the increased colocalization along development is verified for Rpt3 subunit and GluN1 subunit, and not for Rpt3 subunit and PSD-95, could imply that the GluN1 subunit influences the proteasome localization

in spontaneous activity conditions. However, the inverse is also plausible. Nevertheless, since the GluN1 subunit colocalizes with GluN2A and GluN2B subunits along development of cultured rat hippocampal neurons [11], we could extend this hypothesis, needing further clarification, to NMDAR as a whole.

In terms of synaptic localization of the three proteins in question, the Rpt3 subunit and GluN1 subunit accumulate and cluster at synapses in a similar time frame and with similar increasing order of magnitude during development, except at DIV 32 (Figure 10, panels C and D). For matters of puncta quantification synapses were defined exclusively by the presence of the presynaptic protein VGLUT1. PSD-95 accumulates at synapses to a greater extent than the Rpt3 subunit or the GluN1 subunit and suffers minor fluctuations from DIV 5 to 13, after which PSD-95 accumulation increases. The intensity of PSD-95 increases along development except at DIV 13, where oddly synaptic PSD-95 clustering abruptly decreases (Figure 10, panels C and D). However, since this observation corresponds to one single experiment the whole experiment should be reproduced more times.

Also, another intriguing fact, worthy of investigation, is the colocalization or the synaptic localization of the three proteins at DIV 32, which mainly decreases, with the exception of synaptic PSD-95 clustering (Figure 10, panels C and D). This observation could be the result of neuronal senescence at DIV 32 or since we observed excitatory synapse formation, maturation and maintenance in spontaneous activity conditions the hippocampal neurons at DIV 32 could be in a quiescent state characterized by reduced synaptic activity.

Together, these results constitute a starting point for considering the hypothesis that synaptic localization of the proteasome and NMDAR along development of cultured hippocampal neurons may be interdependent.

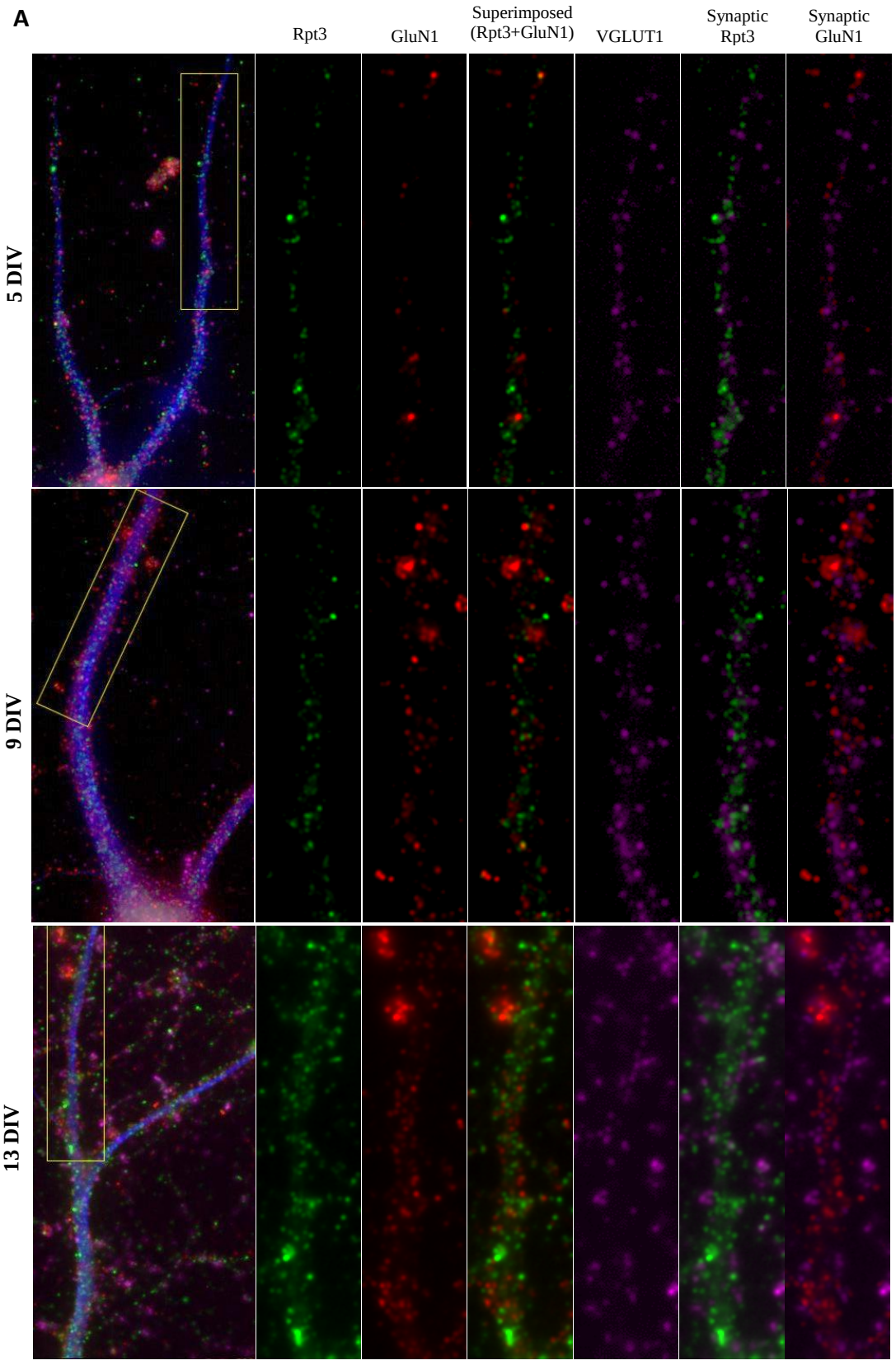
A
Rpt3
GluN1
Superimposed (Rpt3+GluN1)
VGLUT1
Synaptic Rpt3
Synaptic GluN1
5 DIV
9 DIV
13 DIV

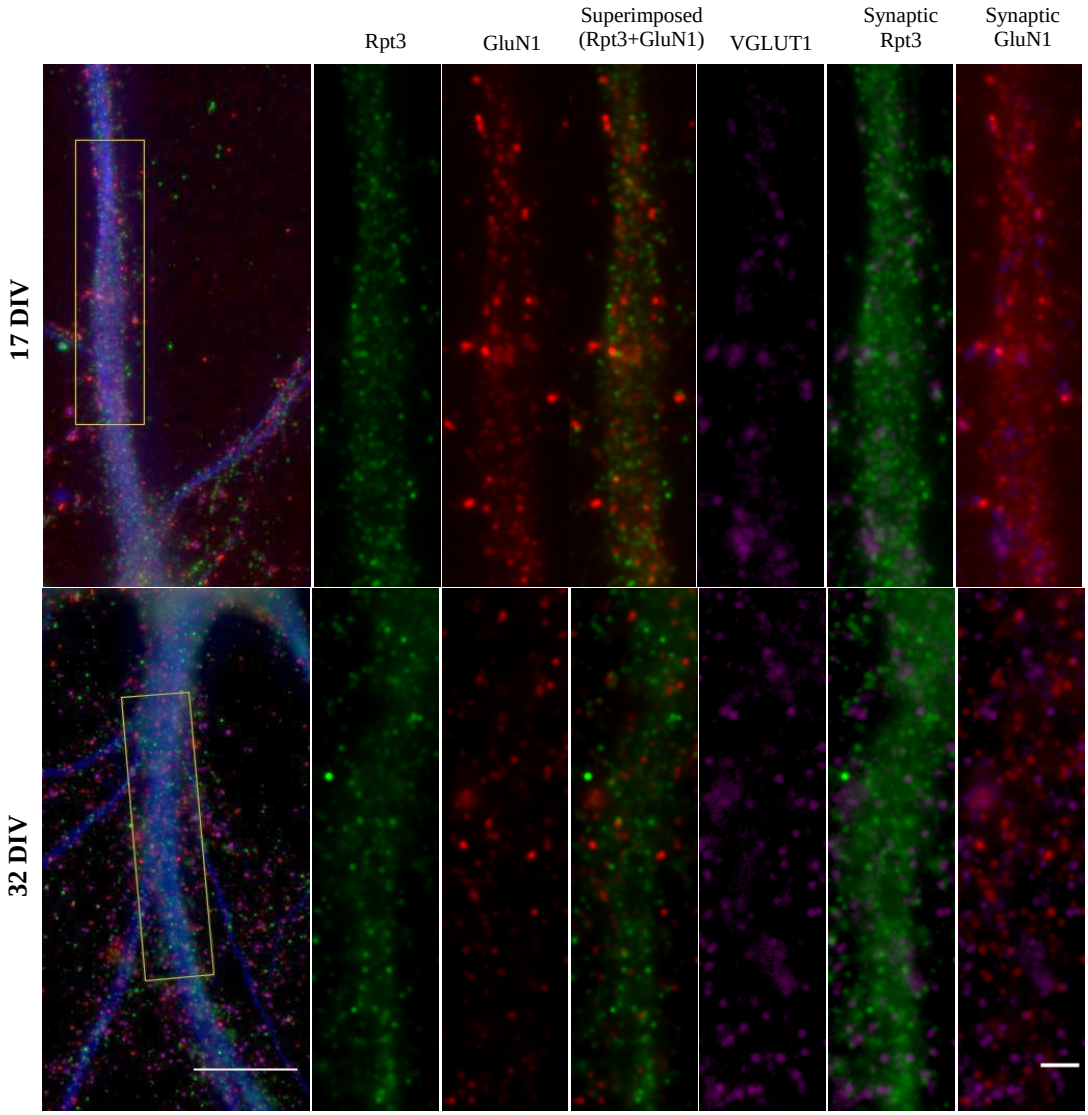
Rpt3
GluN1
Superimposed (Rpt3+GluN1)
VGLUT1
Synaptic Rpt3
Synaptic GluN1
17 DIV
32 DIV

**B**

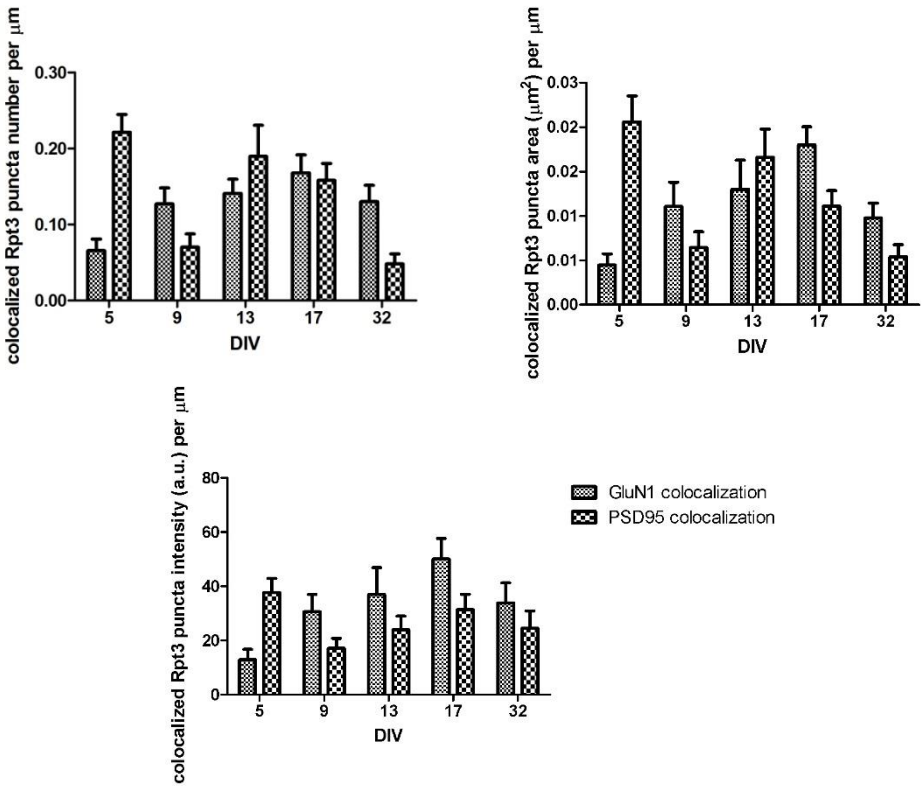
colocalized Rpt3 puncta number per µm
0.30
0.20
0.10
0.00
5
9
13
17
32
DIV
colocalized Rpt3 puncta area (µm²) per µm
0.03
0.02
0.02
0.01
0.01
0.00
5
9
13
17
32
DIV
colocalized Rpt3 puncta intensity (a.u.) per µm
80
60
40
20
0
5
9
13
17
32
DIV
GluN1 colocalization
PSD95 colocalization

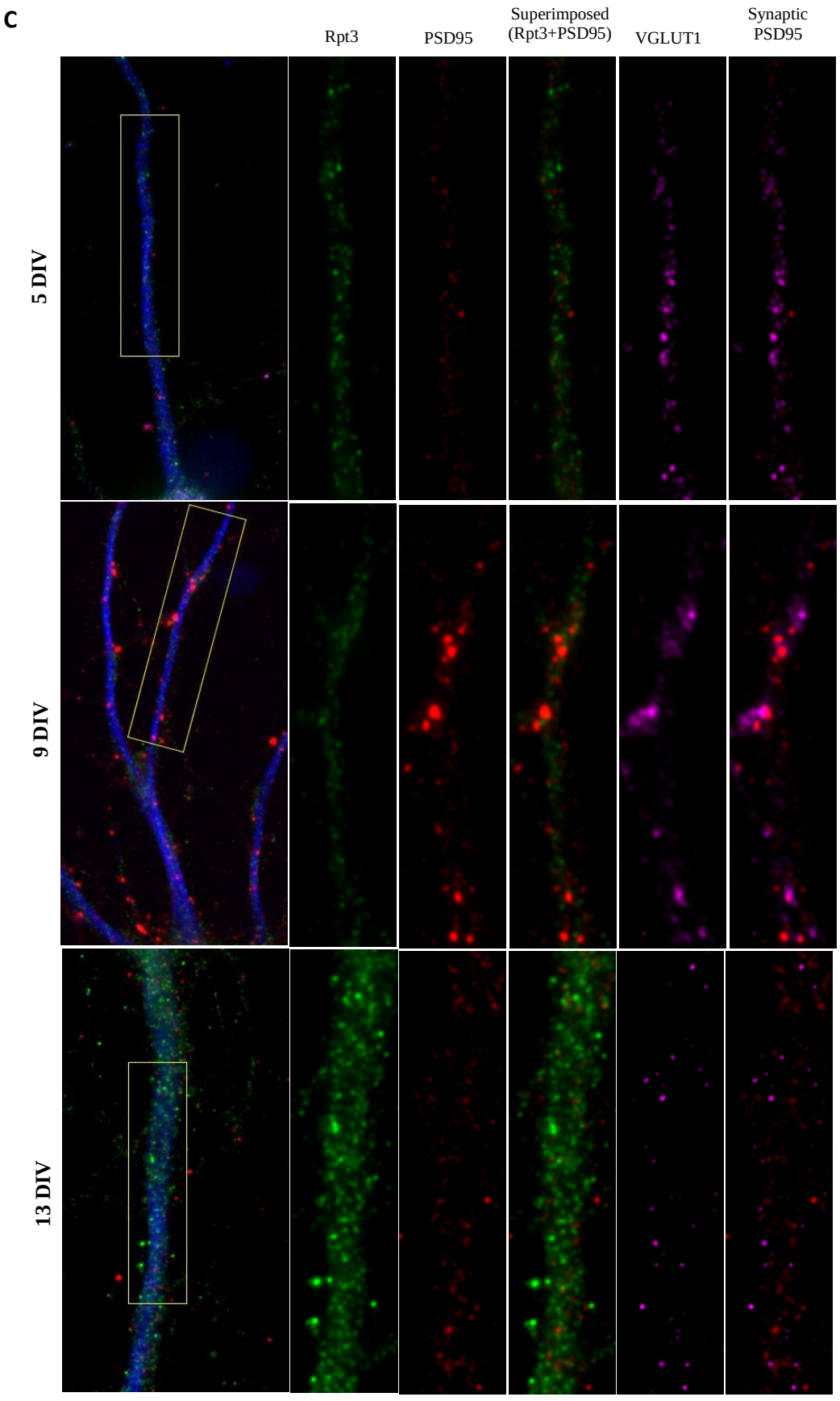
C
Rpt3
PSD95
Superimposed (Rpt3+PSD95)
VGLUT1
Synaptic PSD95
5 DIV
9 DIV
13 DIV

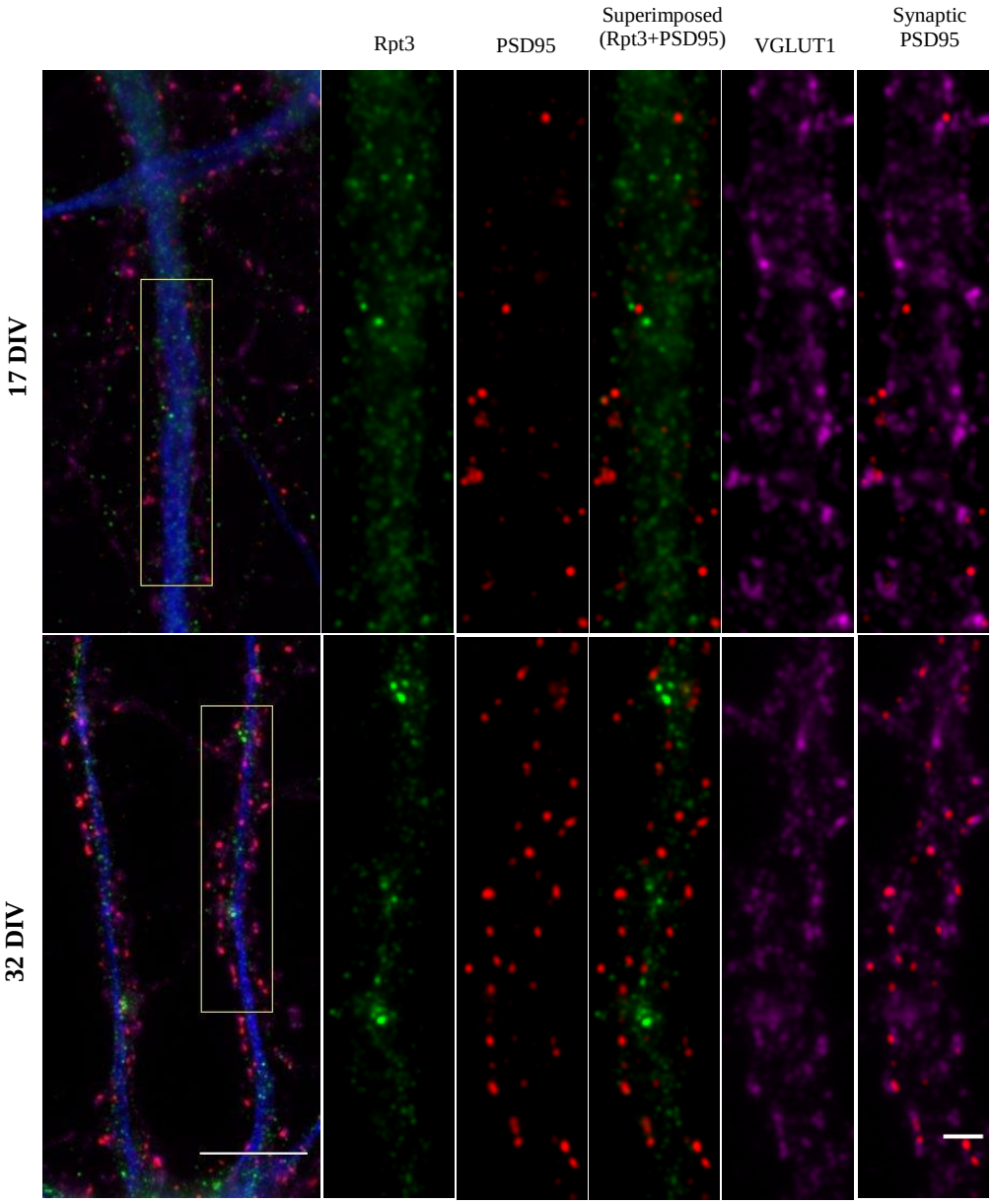
Rpt3
PSD95
Superimposed (Rpt3+PSD95)
VGLUT1
Synaptic PSD95
17 DIV
32 DIV

**D**

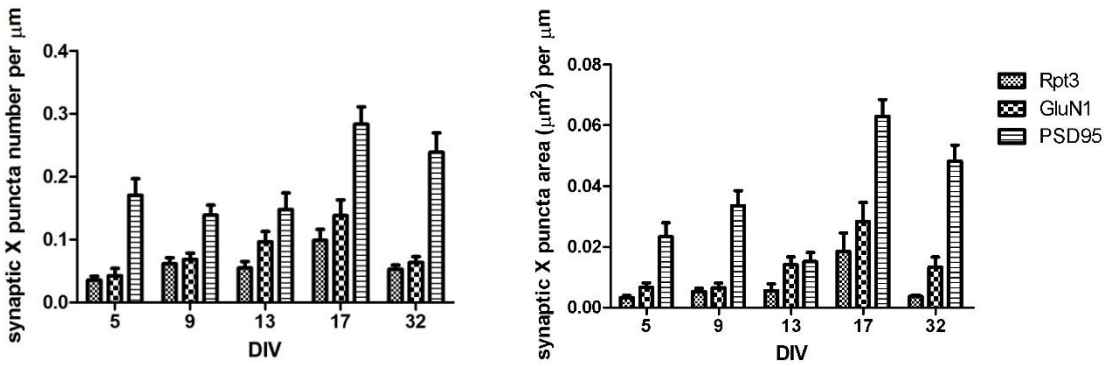
synaptic X puncta number per μm
0.4
0.3
0.2
0.1
0.0
5
9
13
17
32
DIV
synaptic X puncta area (μm²) per μm
0.08
0.06
0.04
0.02
0.00
Rpt3
GluN1
PSD95

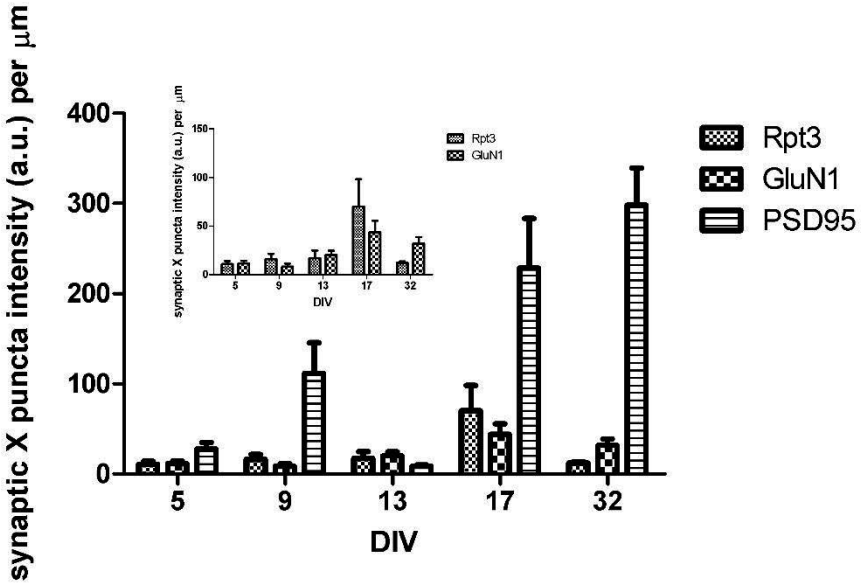


**Figure 10. GluN1 subunit and Rpt3 subunit exhibit similar increasing patterns of localization, in opposition to PSD95, during hippocampal culture development.** Low density cultures of rat hippocampal neurons were fixed at several time points during its development, specifically at 5, 9, 13, 17 and 32 DIV. Since specific immunolabeling of GluN1 subunit is only obtained with methanol fixation and not with paraformaldehyde one, panel **A** and **C** result from methanol and paraformaldehyde fixation, respectively. Following fixation, neurons were immunolabeled for the Rpt3 subunit of the proteasome, the presynaptic protein VGLUT1 and MAP2 (blue signal). Along with the previously mentioned proteins, methanol-and paraformaldehyde-fixed neurons were also labeled for the GluN1 subunit of the NMDA receptors and the postsynaptic protein PSD95, respectively. Two aspects of protein localization were under study, 1) the colocalization between the Rpt3 subunit and the GluN1 subunit or between the Rpt3 subunit and the protein PSD95; and 2) the synaptic localization of the three aforementioned proteins. For quantification matters, the synapse was defined only by the dilated VGLUT1 puncta, which can be seen as a limitation because parts of the area of synapses will be excluded and, by extension, protein puncta localized within the synapse. Scale bar 10 µm; scale bar (crop) 2 µm. Bar graphs **B** and **D** translates the information obtained through puncta quantification. The GluN1 subunit and the Rpt3 subunit colocalization increases along synapse formation and maturation and also these two proteins accumulate and cluster at synapses in a similar time frame and similar increasing order of magnitude. The same is not true for PSD95, because colocalization with Rpt3 subunit oscillates along development and its synaptic localization has a distinct pattern of accumulation and clustering, when compared to Rpt3 subunit and GluN1 subunit. Even being preliminary observations, this interesting fact could mean that the proteasome could be behind the regulation of NMDAR localization during development of cultured hippocampal neurons. Results from puncta quantification are presented as means ± SEM.

## 5. CONCLUSIONS

Preliminary data from our laboratory showed that several 20S proteasome subunits, specifically α1, 3 and 6 and β1 and 2 subunits, are diminished in PSDs isolated from GluN2B(-/-) cortical neurons when compared to GluN2B(+/+) ones. This observation prompted us to investigate the relation between the GluN2B subunit and the proteasome and even elucidate to which level this relation affects the proteasome, knowing from previous studies that upon synaptic activity the proteasome is recruited and sequestered at dendritic spines, where it turned over locally the synaptic proteome [66].

Firstly, we aimed at confirming the diminished synaptic proteasome levels at GluN2B(-/-) PSDs when compared to WT ones through complementary approaches. One approach was to perform WB against the Rpt6 subunit of the proteasome in DIV 14-15 mice cortical membrane extracts. This approach showed no changes in the Rpt6 subunit levels in neurons lacking GluN2B. Nonetheless, this is only one of the many subunits of the 26S proteasome. In addition, since we used total membrane extracts, this approach does not reflect the proteasome content at the postsynaptic side of synapses, or at the PSD fraction, even if the levels of axonal proteasome seem to be smaller than its dendritic levels. Anyhow, we should evaluate the proteasome content in PSD fractions, rather than in whole membrane extracts or even in synaptoneurosomal fractions, by WB against other proteasome subunits. Alternatively or in parallel to WB, we could follow the initial plan of assessing the proteasome endogenous levels at DIV 15 by quantitative immunocytochemistry in low density mice hippocampal cultures because using postsynaptic markers, like PSD-95, we could quantify the synaptic levels of the proteasome. In the case of quantitative immunocytochemistry, the overexpression of Rpt1 subunit was abandoned since the overexpression results in high levels of the protein and makes it impossible to quantify each individual Rpt1-GFP punctum (results not shown).

Secondly, we aimed to determine if GluN2B subunit affects the proteasome activity. To achieve this, proteasome-dependent proteolysis was assessed *in vitro* and in live neurons. Focusing on *in vitro* results, the proteasome activity, extrapolated from the proteasome chymotrypic activity, in mice cortical homogenates with DIV 15-16 is decreased in the absence of the GluN2B subunit. The same is verified using an assay that evaluates proteasome-dependent proteolysis in live neurons, where the GFP-based proteasomal degradation reporter, i.e. the $Ub^{G76V}$-GFP construct, expression at DIV 16 is accumulated when the GluN2B subunit is absent, suggestive of decreased proteasomal

activity. Consequently, this means that the proteasome activity is decreased in GluN2B(-/-) cortical total extracts when compared to control ones. In essence, both approaches convey into the same conclusion that the absence of the GluN2B subunit leads to the decrease of proteasome activity. However, mechanistically it is not fully understood how the GluN2B subunit regulates the proteasome activity. Given that both set of results concerning the proteasome activity are identical and that the fluorogenic substrate suc-LLVY-AMC is degraded independently of ubiquitin tagging while the $Ub^{G76V}$-GFP reporter is not, we can speculate that the explanation is in a downstream event of ubiquitination, maybe in the proteasome itself. αCaMKII, functioning as a kinase, stimulates proteasome activity by posttranslational modifications like the phosphorylation of Rpt6 on serine 120 [65]. Since GluN2B subunit is one of the multiple interaction partners of CaMKII, the synaptic accumulation of CaMKII in response to NMDAR activation is inhibited in part by the GluN2B subunit absence [88]. Therefore, it would be interesting to assess if Rpt6 phosphorylation on serine 120 is affected according to the presence or absence of the GluN2B subunit. If verified, in this scenario of altered phosphorylated Rpt6 levels where the GluN2B subunit would appear? In this line of thought, a rescue approach in GluN2B(-/-) neurons where the GluN2B subunit is overexpressed should restore the proteasome activity to levels similar to the ones seen in GluN2B(+/+) neurons. To ascertain whether the potential recovery in proteasome activity by GluN2B subunit overexpression is dependent on CaMKII, we should use a GluN2B subunit mutant which could abolish the binding of αCaMKII to the high affinity sites on GluN2B subunit. In this way we should be able to unravel whether the GluN2B subunit regulates the proteasome activity via the CaMKII. Either way, the present study shows evidences that the GluN2B subunit affects the proteasome activity in basal activity conditions.

Thirdly, we sought to examine if the mobility of the synaptic proteasome is altered in the absence of the GluN2B subunit. Even though the aim is far from being accomplished, some progress on FRAP optimization has been done. Nevertheless, some limitations still need to be overcome. One will be the imaging chamber since the one used restricts the area of selection i.e. the selection is limited to the center of the coverslip where the percentage of transfected/infected neurons is potentially reduced. Also, some variables fundamental for assessing protein mobility in live neurons have been neglected like the temperature and $CO_2$ control, so this must be changed in order to monitor faithfully the protein dynamics in physiological conditions. Even in these inadequate conditions, we

were capable of seeing fluorescence recovery of the fusion protein EGFP-Rpt1 subunit, which indicates protein mobility occurring under basal synaptic activity. However, in this optimization phase, we could still not test how the GluN2B subunit influences the fluorescence recovery of the protein in question.

The GluN1 subunit and the Rpt3 subunit seem to display similar increasing patterns of localization, synaptic or not, during hippocampal culture development, suggestive of mutual dependency on the dendritic localization of these questions. Some questions remain unanswered as follows: to which extent and by which molecular mechanism(s) is the proteasome involved in PSD remodeling underlying synaptic activity, particularly in terms of NMDAR cycling in and out of synaptic membrane? And during synapse formation and maturation, could the proteasome have a distinct role in NMDAR localization from the one it plays at mature synapses? These questions would allow taking a step forward in understanding if and how the proteasome modulates the NMDAR surface expression, which ultimately could control the synaptic function and plasticity.

Above all, this thesis comprises preliminary experiments which show that the postsynaptic proteasome is affected, at least in its activity by the GluN2B subunit and could be involved in the GluN2B subunit localization during hippocampus development. In my opinion, these interesting observations are worthy of being further clarified because knowing more about the proteasome and its substrates will allow to understand mechanistically and molecularly how the synapse function is controlled and adjusted by local proteasome degradation.

## 6. REFERENCES


[1] H. Husi and S. G. Grant, “Proteomics of the nervous system,” *Trends Neurosci*, vol. 24, no. 5, pp. 259–266, 2001.

[2] V. Haucke, E. Neher, and S. J. Sigrist, “Protein scaffolds in the coupling of synaptic exocytosis and endocytosis,” *Nat Rev Neurosci*, vol. 12, no. 3, pp. 127–138, 2011.

[3] M. Sheng and J. Lin, “Glutamatergic Synapses: Molecular Organization,” *Encycl. Life Sci.*, 2001.

[4] A. N. Hegde, “Ubiquitin-proteasome-mediated local protein degradation and synaptic plasticity,” *Prog Neurobiol*, vol. 73, no. 5, pp. 311–357, 2004.

[5] M. Sheng and C. C. Hoogenraad, “The postsynaptic architecture of excitatory synapses: a more quantitative view.,” *Annu. Rev. Biochem.*, vol. 76, pp. 823–47, Jan. 2007.

[6] C. C. Garner, J. Nash, and R. L. Huganir, “PDZ domains in synapse assembly and signalling.,” *Trends Cell Biol.*, vol. 10, no. 7, pp. 274–80, Jul. 2000.

[7] E. Kim and M. Sheng, “The postsynaptic density,” *Current Biology*, vol. 19, no. 17. pp. R723-4, 15-Sep-2009.

[8] M. Sheng and E. Kim, “The postsynaptic organization of synapses.,” *Cold Spring Harb. Perspect. Biol.*, vol. 3, no. 12, pp. 1–20, Dec. 2011.

[9] H.-C. Kornau, P. H. Seeburg, and M. B. Kennedy, “Interaction of ion channels and receptors with PDZ domain proteins,” *Curr. Opin. Neurobiol.*, vol. 7, no. 3, pp. 368–373, Jun. 1997.

[10] M. Niethammer, E. Kim, and M. Sheng, “Interaction between the C terminus of NMDA receptor subunits and multiple members of the PSD-95 family of membrane-associated guanylate kinases.,” *The Journal of neuroscience : the official journal of the Society for Neuroscience*, vol. 16, no. 7. pp. 2157–63, 01-Apr-1996.

[11] a Rao, E. Kim, M. Sheng, and a M. Craig, “Heterogeneity in the molecular composition of excitatory postsynaptic sites during development of hippocampal neurons in culture.,” *J. Neurosci.*, vol. 18, no. 4, pp. 1217–29, Feb. 1998.

[12] B. Bingol, C.-F. Wang, D. Arnott, D. Cheng, J. Peng, and M. Sheng, “Autophosphorylated CaMKIIalpha acts as a scaffold to recruit proteasomes to dendritic spines.,” *Cell*, vol. 140, no. 4, pp. 567–78, Feb. 2010.

[13] J. Lisman, H. Schulman, and H. Cline, “The molecular basis of CaMKII function in synaptic and behavioural memory.,” *Nat. Rev. Neurosci.*, vol. 3, no. 3, pp. 175–90, Mar. 2002.

[14] R. J. Colbran, “Targeting of calcium/calmodulin-dependent protein kinase II.,” *Biochem. J.*, vol. 378, no. Pt 1, pp. 1–16, Feb. 2004.

[15] J. Lisman, R. Yasuda, and S. Raghavachari, “Mechanisms of CaMKII action in long-term potentiation.,” *Nat. Rev. Neurosci.*, vol. 13, no. 3, pp. 169–82, Mar. 2012.

[16] M. a Merrill, Y. Chen, S. Strack, and J. W. Hell, “Activity-driven postsynaptic translocation of CaMKII.,” *Trends Pharmacol. Sci.*, vol. 26, no. 12, pp. 645–53, Dec. 2005.

[17] J. W. Hell, “CaMKII: claiming center stage in postsynaptic function and organization.,” *Neuron*, vol. 81, no. 2, pp. 249–65, Jan. 2014.

[18] K.-I. Okamoto, R. Narayanan, S. H. Lee, K. Murata, and Y. Hayashi, “The role of CaMKII as an F-actin-bundling protein crucial for maintenance of dendritic spine structure.,” *Proc. Natl. Acad. Sci. U. S. A.*, vol. 104, no. 15, pp. 6418–23, Apr. 2007.

[19] B. Xiao *et al.*, “Homer regulates the association of group 1 metabotropic glutamate receptors with multivalent complexes of homer-related, synaptic proteins.,” *Neuron*, vol. 21, no. 4, pp. 707–16, Oct. 1998.

[20] M. H. Glickman and A. Ciechanover, “The ubiquitin-proteasome proteolytic pathway: destruction for the sake of construction.,” *Physiol. Rev.*, vol. 82, no. 2, pp. 373–428, Apr. 2002.

[21] a Hershko and a Ciechanover, “The ubiquitin system.,” *Annu. Rev. Biochem.*, vol. 67, pp. 425–79, Jan. 1998.

[22] A. W. Lin and H.-Y. Man, “Ubiquitination of neurotransmitter receptors and postsynaptic scaffolding proteins.,” *Neural Plast.*, vol. 2013, no. Figure 1, p. 432057, Jan. 2013.

[23] C.-W. Liu and A. D. Jacobson, “Functions of the 19S complex in proteasomal degradation.,” *Trends Biochem. Sci.*, vol. 38, no. 2, pp. 103–10, Feb. 2013.

[24] D. Voges, P. Zwickl, and W. Baumeister, “The 26S proteasome: a molecular machine designed for controlled proteolysis.,” *Annu. Rev. Biochem.*, vol. 68, pp. 1015–68, Jan. 1999.

[25] R. J. Tomko and M. Hochstrasser, “Molecular architecture and assembly of the eukaryotic proteasome.,” *Annu. Rev. Biochem.*, vol. 82, pp. 415–45, Jan. 2013.

[26] A. F. Kisselev, T. N. Akopian, V. Castillo, and A. L. Goldberg, “Proteasome active sites allosterically regulate each other, suggesting a cyclical bite-chew mechanism for protein breakdown.,” *Mol. Cell*, vol. 4, no. 3, pp. 395–402, Sep. 1999.

[27] G. C. Lander, E. Estrin, M. E. Matyskiela, C. Bashore, E. Nogales, and A. Martin, “Complete subunit architecture of the proteasome regulatory particle.,” *Nature*, vol. 482, no. 7384, pp. 186–91, Feb. 2012.

[28] A. N. Hegde, “The ubiquitin-proteasome pathway and synaptic plasticity.,” *Learn. Mem.*, vol. 17, no. 7, pp. 314–27, Jul. 2010.

[29] P. Paoletti, C. Bellone, and Q. Zhou, “NMDA receptor subunit diversity: impact on receptor properties, synaptic plasticity and disease.,” *Nat. Rev. Neurosci.*, vol. 14, no. 6, pp. 383–400, Jun. 2013.

[30] S. G. Cull-Candy, “NMDA Receptors,” *Encycl. Life Sci.*, 2007.

[31] R. C. Carroll and R. S. Zukin, “NMDA-receptor trafficking and targeting: implications for synaptic transmission and plasticity.,” *Trends Neurosci.*, vol. 25, no. 11, pp. 571–7, Nov. 2002.

[32] P. Paoletti, “Molecular basis of NMDA receptor functional diversity.,” *Eur. J. Neurosci.*, vol. 33, no. 8, pp. 1351–65, Apr. 2011.

[33] S. F. Traynelis *et al.*, “Glutamate receptor ion channels: structure, regulation, and function.,” *Pharmacol. Rev.*, vol. 62, no. 3, pp. 405–96, Sep. 2010.

[34] D. J. a Wyllie, M. R. Livesey, and G. E. Hardingham, “Influence of GluN2 subunit

identity on NMDA receptor function.," *Neuropharmacology*, vol. 74, pp. 4–17, Nov. 2013.

[35] G. E. Hardingham and H. Bading, "The Yin and Yang of NMDA receptor signalling," *Trends Neurosci.*, vol. 26, no. 2, pp. 81–89, 2003.

[36] G. E. Hardingham and H. Bading, "Synaptic versus extrasynaptic NMDA receptor signalling: implications for neurodegenerative disorders.," *Nat. Rev. Neurosci.*, vol. 11, no. 10, pp. 682–96, Oct. 2010.

[37] M.-A. Martel *et al.*, "The subtype of GluN2 C-terminal domain determines the response to excitotoxic insults.," *Neuron*, vol. 74, no. 3, pp. 543–56, May 2012.

[38] M. Martel, D. J. A. Wyllie, and G. E. Hardingham, "In developing hippocampal neurons, NR2B-containing N-methyl-D-aspartate receptors (NMDARs) can mediate signaling to neuronal survival and synaptic potentiation, as well as neuronal death.," *Neuroscience*, vol. 158, no. 1, pp. 334–43, Jan. 2009.

[39] Q. Zhou and M. Sheng, "NMDA receptors in nervous system diseases," *Neuropharmacology*, vol. 74, pp. 69–75, 2013.

[40] A. Sanz-Clemente, R. a Nicoll, and K. W. Roche, "Diversity in NMDA receptor composition: many regulators, many consequences.," *Neuroscientist*, vol. 19, no. 1, pp. 62–75, Mar. 2013.

[41] B. Bingol and M. Sheng, "Deconstruction for reconstruction: the role of proteolysis in neural plasticity and disease.," *Neuron*, vol. 69, no. 1, pp. 22–32, Jan. 2011.

[42] A. M. Mabb and M. D. Ehlers, "Ubiquitination in postsynaptic function and plasticity.," *Annu. Rev. Cell Dev. Biol.*, vol. 26, pp. 179–210, Jan. 2010.

[43] M. D. Ehlers, "Activity level controls postsynaptic composition and signaling via the ubiquitin-proteasome system.," *Nat. Neurosci.*, vol. 6, no. 3, pp. 231–42, Mar. 2003.

[44] J. Lisman, "Glutamatergic synapses are structurally and biochemically complex because of multiple plasticity processes: Long-term potentiation, long-term depression, short-term potentiation and scaling," *Philos. Trans. R. Soc. B Biol. Sci.*, vol. 372, no. 1715, 2017.

[45] I. Pérez-Otaño and M. D. Ehlers, "Homeostatic plasticity and NMDA receptor trafficking," *Trends Neurosci.*, vol. 28, no. 5, pp. 229–238, 2005.

[46] A. Volianskis, G. France, M. S. Jensen, Z. A. Bortolotto, D. E. Jane, and G. L. Collingridge, "Long-term potentiation and the role of N-methyl-D-aspartate receptors," *Brain Res.*, vol. 1621, pp. 5–16, 2015.

[47] A. N. Hegde, "Proteolysis, synaptic plasticity and memory," *Neurobiol. Learn. Mem.*, vol. 138, no. 8, pp. 98–110, Feb. 2017.

[48] R. C. Malenka and M. F. Bear, "LTP and LTD: An embarrassment of riches," *Neuron*, vol. 44, no. 1, pp. 5–21, 2004.

[49] S. D. Santos, A. L. Carvalho, M. V. Caldeira, and C. B. Duarte, "Regulation of AMPA receptors and synaptic plasticity," *Neuroscience*, vol. 158, no. 1, pp. 105–125, 2009.

[50] A. Barria and R. Malinow, "NMDA receptor subunit composition controls synaptic plasticity by regulating binding to CaMKII.," *Neuron*, vol. 48, no. 2, pp. 289–301, Oct. 2005.

[51] R. Yuste and T. Bonhoeffer, “Morphological changes in dendritic spines associated with long-term synaptic plasticity,” *Annu. Rev. Neurosci.*, vol. 24, no. 1862, pp. 1071–89, Jan. 2001.

[52] C. Lüscher, R. a Nicoll, R. C. Malenka, and D. Muller, “Synaptic plasticity and dynamic modulation of the postsynaptic membrane.,” *Nat. Neurosci.*, vol. 3, no. 6, pp. 545–50, Jun. 2000.

[53] R. K. Murphey and T. a Godenschwege, “New roles for ubiquitin in the assembly and function of neuronal circuits.,” *Neuron*, vol. 36, no. 1, pp. 5–8, Sep. 2002.

[54] A. DiAntonio, A. P. Haghighi, S. L. Portman, J. D. Lee, A. M. Amaranto, and C. S. Goodman, “Ubiquitination-dependent mechanisms regulate synaptic growth and function.,” *Nature*, vol. 412, no. 6845, pp. 449–52, Jul. 2001.

[55] K. Shen and T. Meyer, “Dynamic control of CaMKII translocation and localization in hippocampal neurons by NMDA receptor stimulation.,” *Science*, vol. 284, no. 5411, pp. 162–6, Apr. 1999.

[56] T. Meyer and K. Shen, “In and out of the postsynaptic region: signalling proteins on the move,” *Trends in Cell Biology*, vol. 10, no. 6. pp. 238–244, Jun-2000.

[57] S. Okabe, H. D. Kim, a Miwa, T. Kuriu, and H. Okado, “Continual remodeling of postsynaptic density and its regulation by synaptic activity.,” *Nat. Neurosci.*, vol. 2, no. 9, pp. 804–11, Sep. 1999.

[58] G. S. Marrs, S. H. Green, and M. E. Dailey, “Rapid formation and remodeling of postsynaptic densities in developing dendrites.,” *Nat. Neurosci.*, vol. 4, no. 10, pp. 1006–13, Oct. 2001.

[59] S. Strack, “Autophosphorylation-dependent Targeting of Calcium/ Calmodulin-dependent Protein Kinase II by the NR2B Subunit of the N-Methyl- D-aspartate Receptor,” *J. Biol. Chem.*, vol. 273, no. 33, pp. 20689–20692, Aug. 1998.

[60] M. Mayadevi, M. Praseeda, K. S. Kumar, and R. V Omkumar, “Sequence determinants on the NR2A and NR2B subunits of NMDA receptor responsible for specificity of phosphorylation by CaMKII.,” *Biochim. Biophys. Acta*, vol. 1598, no. 1–2, pp. 40–5, Jul. 2002.

[61] G. Köhr *et al.*, “Intracellular domains of NMDA receptor subtypes are determinants for long-term potentiation induction.,” *J. Neurosci.*, vol. 23, no. 34, pp. 10791–9, Nov. 2003.

[62] Y. Zhou *et al.*, “Interactions between the NR2B receptor and CaMKII modulate synaptic plasticity and spatial learning.,” *J. Neurosci.*, vol. 27, no. 50, pp. 13843–53, Dec. 2007.

[63] F. Zhang, A. J. Paterson, P. Huang, K. Wang, and J. E. Kudlow, “Metabolic control of proteasome function.,” *Physiology (Bethesda).*, vol. 22, pp. 373–9, Dec. 2007.

[64] M. H. Glickman and D. Raveh, “Proteasome plasticity.,” *FEBS Lett.*, vol. 579, no. 15, pp. 3214–23, Jun. 2005.

[65] S. N. Djakovic, L. a Schwarz, B. Barylko, G. N. DeMartino, and G. N. Patrick, “Regulation of the proteasome by neuronal activity and calcium/calmodulin-dependent protein kinase II.,” *J. Biol. Chem.*, vol. 284, no. 39, pp. 26655–65, Sep. 2009.

[66] B. Bingol and E. M. Schuman, “Activity-dependent dynamics and sequestration of proteasomes in dendritic spines.,” *Nature*, vol. 441, no. 7097, pp. 1144–8, Jun.

2006.

[67] J. Rose, S. Jin, and A. Craig, “Heterosynaptic molecular dynamics: locally induced propagating synaptic accumulation of CaM kinase II,” *Neuron*, vol. 61, no. 3, pp. 351–8, Feb. 2009.

[68] S. N. Djakovic *et al.*, “Phosphorylation of Rpt6 regulates synaptic strength in hippocampal neurons.,” *J. Neurosci.*, vol. 32, no. 15, pp. 5126–31, Apr. 2012.

[69] J. S. Ferreira *et al.*, “GluN2B-Containing NMDA Receptors Regulate AMPA Receptor Traffic through Anchoring of the Synaptic Proteasome.,” *J. Neurosci.*, vol. 35, no. 22, pp. 8462–79, 2015.

[70] T. Kutsuwada *et al.*, “Impairment of suckling response, trigeminal neuronal pattern formation, and hippocampal LTD in NMDA receptor epsilon 2 subunit mutant mice.,” *Neuron*, vol. 16, no. 2. pp. 333–44, Mar-1996.

[71] K. R. Tovar, K. Sprouffske, and G. L. Westbrook, “Fast NMDA receptor-mediated synaptic currents in neurons from mice lacking the epsilon2 (NR2B) subunit.,” *J. Neurophysiol.*, vol. 83, no. 1, pp. 616–20, Jan. 2000.

[72] G. Goslin, K., Asmussen, H. & Banker, “Rat hippocampal neurons in low-density cultures,” in *Culturing Nerve Cells*, K. Banker, G. & Goslin, Ed. The MIT Press, Cambridge, Massachusetts, USA, 1998, pp. 339–370.

[73] S. Kaech and G. Banker, “Culturing hippocampal neurons.,” *Nat. Protoc.*, vol. 1, no. 5, pp. 2406–15, Jan. 2006.

[74] J. S. Ferreira, A. Rooyakkers, K. She, L. Ribeiro, A. L. Carvalho, and A. M. Craig, “Activity and protein kinase C regulate synaptic accumulation of N-methyl-D-aspartate (NMDA) receptors independently of GluN1 splice variant.,” *J. Biol. Chem.*, vol. 286, no. 32, pp. 28331–42, Aug. 2011.

[75] C. Y. Shin, M. Kundel, and D. G. Wells, “Rapid, activity-induced increase in tissue plasminogen activator is mediated by metabotropic glutamate receptor-dependent mRNA translation.,” *J. Neurosci.*, vol. 24, no. 42, pp. 9425–33, Oct. 2004.

[76] M. V Caldeira *et al.*, “Excitotoxic stimulation downregulates the ubiquitin-proteasome system through activation of NMDA receptors in cultured hippocampal neurons.,” *Biochim. Biophys. Acta*, vol. 1832, no. 1, pp. 263–74, Jan. 2013.

[77] M. Jiang, L. Deng, and G. Chen, “High Ca(2+)-phosphate transfection efficiency enables single neuron gene analysis.,” *Gene Ther.*, vol. 11, no. 17, pp. 1303–11, Sep. 2004.

[78] S. Speese, N. Trotta, and C. Rodesch, “The ubiquitin proteasome system acutely regulates presynaptic protein turnover and synaptic efficacy,” *Curr. Biol.*, vol. 13, pp. 899–910, 2003.

[79] L. Villasana, E. Klann, and M. Tejada-Simon, “Rapid isolation of synaptoneurosomes and postsynaptic densities from adult mouse hippocampus,” *J. Neurosci. …*, vol. 158, no. 1, pp. 30–6, Nov. 2006.

[80] P. R. Westmark, C. J. Westmark, A. Jeevananthan, and J. S. Malter, “Preparation of synaptoneurosomes from mouse cortex using a discontinuous percoll-sucrose density gradient.,” *J. Vis. Exp.*, no. 55, pp. 1–9, Jan. 2011.

[81] L. Thomas *et al.*, “Identification of synaptophysin as a hexameric channel protein of the synaptic vesicle membrane.,” *Science*, vol. 242, no. 4881, pp. 1050–3, Nov.

1988.

[82] E. Kim and M. Sheng, “PDZ domain proteins of synapses.,” *Nat. Rev. Neurosci.*, vol. 5, no. 10, pp. 771–81, Oct. 2004.

[83] R. D. Goldman, Y. Gruenbaum, R. D. Moir, D. K. Shumaker, and T. P. Spann, “Nuclear lamins: building blocks of nuclear architecture.,” *Genes Dev.*, vol. 16, no. 5, pp. 533–47, Mar. 2002.

[84] K. S. Kosik and E. a Finch, “MAP2 and tau segregate into dendritic and axonal domains after the elaboration of morphologically distinct neurites: an immunocytochemical study of cultured rat cerebrum.,” *J. Neurosci.*, vol. 7, no. 10, pp. 3142–53, Oct. 1987.

[85] N. P. Dantuma, K. Lindsten, R. Glas, M. Jellne, and M. G. Masucci, “Short-lived green fluorescent proteins for quantifying ubiquitin/proteasome-dependent proteolysis in living cells.,” *Nat. Biotechnol.*, vol. 18, no. 5, pp. 538–43, May 2000.

[86] V. Menéndez-Benito, S. Heessen, and N. P. Dantuma, “Monitoring of ubiquitin-dependent proteolysis with green fluorescent protein substrates.,” *Methods Enzymol.*, vol. 399, no. 2001, pp. 490–511, Jan. 2005.

[87] J. Hanna, A. Meides, D. P. Zhang, and D. Finley, “A ubiquitin stress response induces altered proteasome composition.,” *Cell*, vol. 129, no. 4, pp. 747–59, May 2007.

[88] K. She, J. K. Rose, and A. M. Craig, “Differential stimulus-dependent synaptic recruitment of CaMKIIα by intracellular determinants of GluN2B.,” *Mol. Cell. Neurosci.*, vol. 51, no. 3–4, pp. 68–78, Nov. 2012.